Stem Cell Reports
Article

ISSCR

OPEN ACCESS

Lovastatin promotes the self-renewal of murine and primate spermatogonial stem cells

Chaohui Li,[1,2,12] Zhaokai Yao,[2,12] Linzi Ma,[2,3,12] Xiuling Song,[2,12] Wen Wang,[2] Cong Wan,[2] Shaofang Ren,[2] Dingyao Chen,[2] Yi Zheng,[2] Yong-tong Zhu,[3] Gang Chang,[4] Shihao Wu,[1] Kai Miao,[5,*] Fang Luo,[2,*] and Xiao-Yang Zhao[2,6,7,8,9,10,11,*]

[1]Shunde Hospital of Southern Medical University, Shunde, Guangdong, China
[2]State Key Laboratory of Organ Failure Research, Department of Developmental Biology, School of Basic Medical Sciences, Southern Medical University, Guangzhou, Guangdong, China
[3]Reproductive Medicine Center, Department of Obstetrics and Gynecology, Nanfang Hospital, Southern Medical University, Guangzhou, China
[4]Department of Biochemistry and Molecular Biology, Shenzhen University Health Science Center, Shenzhen, Guangdong, China
[5]Centre for Precision Medicine Research and Training, Faculty of Health Sciences, University of Macau, Macau, SAR, China
[6]Guangdong Provincial Key Laboratory of Construction and Detection in Tissue Engineering, Southern Medical University, Guangzhou, Guangdong, China
[7]Bioland Laboratory (Guangzhou Regenerative Medicine and Health Guangdong Laboratory), Guangzhou, China
[8]Sino-America Joint Research Center for Translational Medicine in Developmental Disabilities, Guangzhou, China
[9]Department of Gynecology, Zhujiang Hospital, Southern Medical University, Guangzhou, Guangdong, China
[10]National Clinical Research Canter for Kidney Disease, Guangzhou, China
[11]Key Laboratory of Mental Health of the Ministry of Education, Guangzhou, China
[12]These authors contributed equally
*Correspondence: kaimiao@umac.mo (K.M.), akidreams@smu.edu.cn (F.L.), zhaoxiaoyang@smu.edu.cn (X.-Y.Z.)
https://doi.org/10.1016/j.stemcr.2023.02.011

SUMMARY

The spermatogonial stem cell (SSC) niche is critical for SSC maintenance and subsequent spermatogenesis. Numerous reproductive hazards impair the SSC niche, thereby resulting in aberrant SSC self-renewal and male infertility. However, promising agents targeting the impaired SSC niche to promote SSC self-renewal are still limited. Here, we screen out and assess the effects of Lovastatin on the self-renewal of mouse SSCs (mSSCs). Mechanistically, Lovastatin promotes the self-renewal of mSSCs and inhibits its inflammation and apoptosis through the regulation of isoprenoid intermediates. Remarkably, treatment by Lovastatin could promote the proliferation of undifferentiated spermatogonia in the male gonadotoxicity model generated by busulfan injection. Of note, we demonstrate that Lovastatin could enhance the proliferation of primate undifferentiated spermatogonia. Collectively, our findings uncover that lovastatin could promote the self-renewal of both murine and primate SSCs and have implications for the treatment of certain types of male infertility using small compounds.

INTRODUCTION

In mammals, spermatogonial stem cells (SSCs) maintain life-long male fertility through a balance between self-renewal and differentiation (Clermont, 1972; de Rooij, 2017; Fayomi and Orwig, 2018). The testicular microenvironment, which is composed of various somatic cells and their secreted growth factors, is critical for the maintenance of SSCs and subsequent spermatogenic differentiation (Chen and Liu, 2015; Mei et al., 2015; Oatley and Brinster, 2012; Tian et al., 2019). Among these growth factors, GDNF, which is secreted by Sertoli and myoid cells, is essential for the self-renewal of SSCs, and the number of SSCs in *GDNF* knockout mice decreased significantly (Chen et al., 2016; Meng et al., 2000; Parekh et al., 2019; Sada et al., 2012; Takashima et al., 2015). The involvement of cytokines in regulating SSC identity lays a foundation for the establishment of an SSC *in vitro* culture system (Kanatsu-Shinohara et al., 2003, 2005, 2011). The widely used mouse SSC (mSSC) *in vitro* culture system contains cytokines such as GDNF, FGF2, LIF, and EGF, which can maintain the long-term expansion of mSSCs; meanwhile, the cultured mSSCs could initiate meiosis properly under induction. More importantly, the long-term cultured mSSCs can produce functional spermatozoa after transplantation into the seminiferous tubules of recipient mice, indicating that growth factors from the testicular microenvironment play an important role in the proper maintenance of SSC identity *in vitro* (Kanatsu-Shinohara et al., 2003; Kubota et al., 2004; Kubota and Brinster, 2018).

However, clinical treatment technologies with reproductive toxicity such as radiotherapy and chemotherapy can damage the testicular microenvironment and impair the SSC pool, thereby resulting in male infertility (Allen et al., 2018; Delessard et al., 2020; Meistrich, 1993, 2013; Vakalopoulos et al., 2015). Previous studies have shown that busulfan chemotherapy, in which a large number of germ cells undergo apoptosis, could decrease the number of mSSCs, undifferentiated spermatogonia, and more differentiated progenitor-type spermatogonia significantly (Liu et al., 2014; Marcon et al., 2010; Nurmio et al., 2009; Zohni et al., 2012). As for the microenvironment, the number of peritubular myoid cells decreased, while malfunction alterations of Leydig cells and Sertoli cells have been

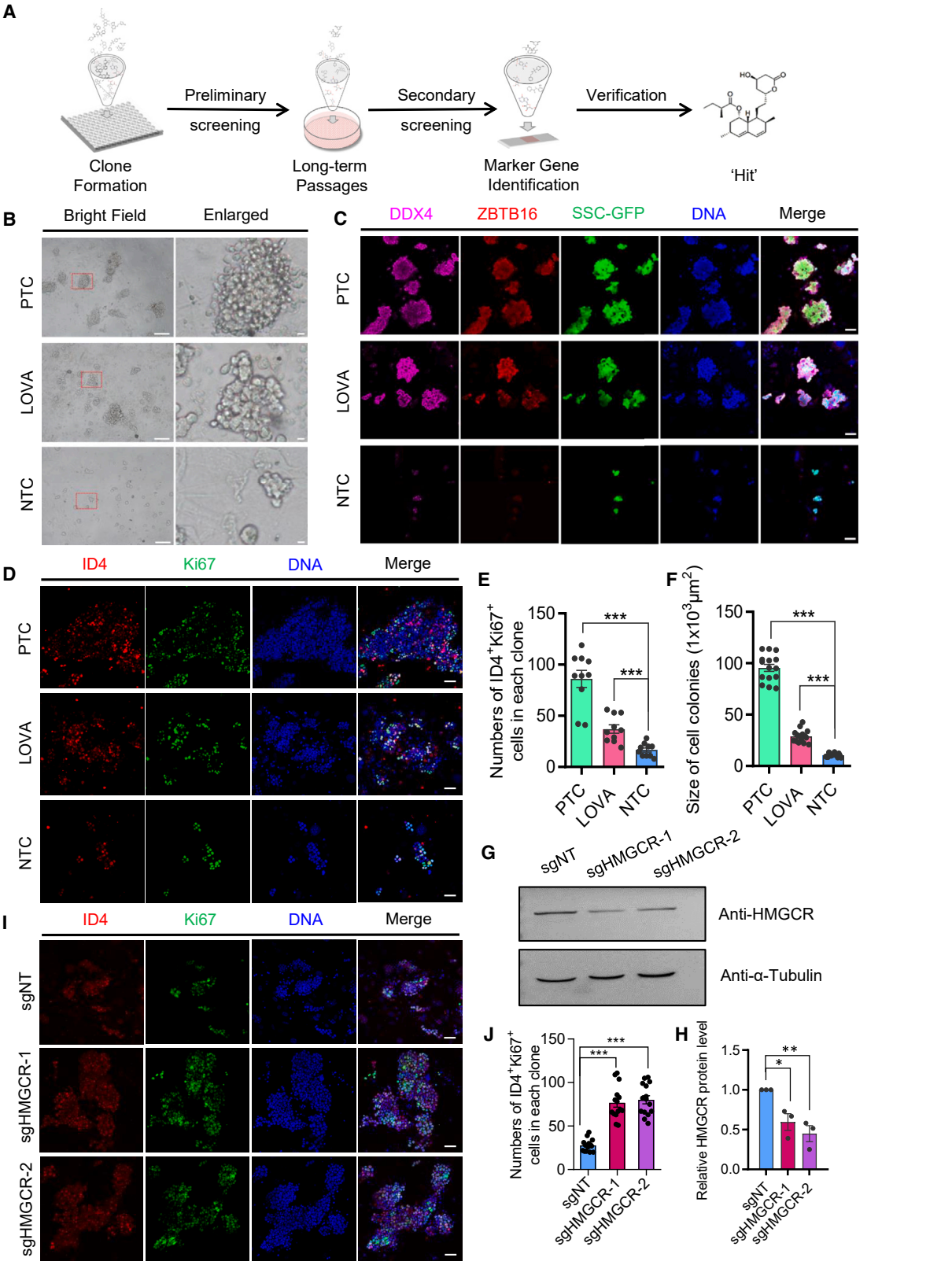

(legend on next page)

reported (Brilhante et al., 2012; Sasso-Cerri et al., 2017) in which the decrease of GDNF was observed (Morimoto et al., 2021). Further studies indicate that proper SSC pools and microenvironments are the basis for restoring male fertility (Benavides-Garcia et al., 2015; Chen et al., 2021; Kotzur et al., 2017; Zhang et al., 2019). Hence, it is of significance to know how to restore the male fertility capability by triggering the proliferation of SSCs under the spermatogenesis defective condition caused by chemotherapy or other reasons.

In this study, we applied a small-compound screening strategy to find a novel small compound that can promote the self-renewal of SSCs using the mSSC *in vitro* culture system without the addition of GDNF. Then, the effects of the candidate small compound were evaluated using both the mouse male infertility model induced by busulfan and the *ex vivo* primate testis culture system.

RESULTS

Small-compound screening identifies that Lovastatin promotes mSSC self-renewal in the absence of GDNF *in vitro*

GDNF is an essential factor for SSC maintenance. To screen novel small compounds that support the long-term maintenance of SSCs, high-throughput screening of small-compound libraries was performed using the *in vitro* mSSC culture system (Figures 1A and S1A). First, we defined two culture conditions for classical mSSC culture medium according to the previous description, which was supplemented with GDNF, FGF2, LIF, and EGF (positive control group [PTC]) (Kanatsu-Shinohara et al., 2003) or PTC without GDNF (negative control group [NTC]), respectively. We then set up the screening system to evaluate the performance of small compounds on the proliferation of mSSCs based on NTC culture conditions. As a result, we screened out a small molecule drug, Lovastatin, which is referred to LOVA hereafter. Similar to PTC, cells from the LOVA group also showed the typical mSSC morphology (Figure 1B). Remarkably, cell clones from both PTC and LOVA groups expressed the germ cell marker DDX4 and undifferentiated spermatogonia marker ZBTB16, which could maintain their expression for 18 days, whereas cell clones from the NTC group barely expressed these markers (Figure 1C). Furthermore, the number of proliferative mSSCs, which was indicated by ID4 (Chan et al., 2014; Sun et al., 2015) and Ki67 double immunostaining, was significantly higher in the LOVA group than in the NTC group, indicating that the supplementation of LOVA significantly promoted proliferation of mSSCs (Figures 1D and 1E). Likewise, the sizes of the cell colonies from the LOVA group were prominently larger than those from the NTC group (Figure 1F). Consistently, mSSCs in the LOVA group showed a tendency toward stable proliferation compared with the NTC group, suggesting that LOVA supports GDNF-independent proliferation of mSSCs (Figure S1B). In addition, we optimized the dosage of LOVA for

Figure 1. Lovastatin maintains the identity of mSSCs *in vitro* in the absence of GDNF

(A) Schematic outline of the small-molecule screening.

(B) Morphology of mSSC clones in different culture conditions. mSSCs cultured in regular conditions that contain exogenous GDNF were named the positive control group (PTC). mSSCs cultured without GDNF were used as the negative control group (NTC). Small-molecule compound-treated mSSC group (Lovastatin [LOVA]) was cultured in NTC medium supplemented with LOVA. The right panel shows the clone enlarged in the red rectangle of left field. Scale bars: left, 100 μm, and right, 10 μm.

(C) Immunofluorescent staining of mSSC clones cultured in different groups for 18 days. GFP indicates mSSC clones seeded in the culture dish. DDX4 and ZBTB16 as germ cell and undifferentiated spermatogonia markers were labeled, respectively. Scale bars, 50 μm.

(D) Immunofluorescent staining of mSSC clones cultured in different groups for 18 days. ID4 and Ki67 as mSSCs and cell proliferation markers were labeled, respectively. Scale bars, 50 μm.

(E) Statistic histogram of ID4 and Ki67 double-positive cells for each group from ten independent experiments. Error bars indicate mean ± SEM, ***$p \leq 0.001$.

(F) Statistic histogram of size of mSSC clones for each group from fifteen independent experiments. Error bars indicate mean ± SEM, ***$p \leq 0.001$.

(G) Western blot of HMGCR knockdown mediated by CRISPR-Cas13d system. sgHMGCR-1 and sgHMGCR-2 were designed to knock down HMGCR, while sgNT indicates non-targeting sgRNA. α-Tubulin was used as the loading control.

(H) Statistic histogram of relative HMGCR protein level in (G) from three independent experiments. Error bars indicate mean ± SEM, *$p \leq 0.05$, **$p \leq 0.01$.

(I) Immunofluorescent staining of HMGCR knockdown and control sgNT mSSCs clones used in (G). mSSC samples were cultured withouth GDNF for 3 passages (18 days) after HMGCR or sgNT knockdown. ID4 and Ki67 as mSSCs and cell proliferation markers were labeled, respectively. Scale bars, 50 μm.

(J) Statistic histogram of ID4 and Ki67 double-positive cells for each group in (I) from ten independent experiments. Error bars indicate mean ± SEM, ***$p \leq 0.001$.

See also Figure S1.

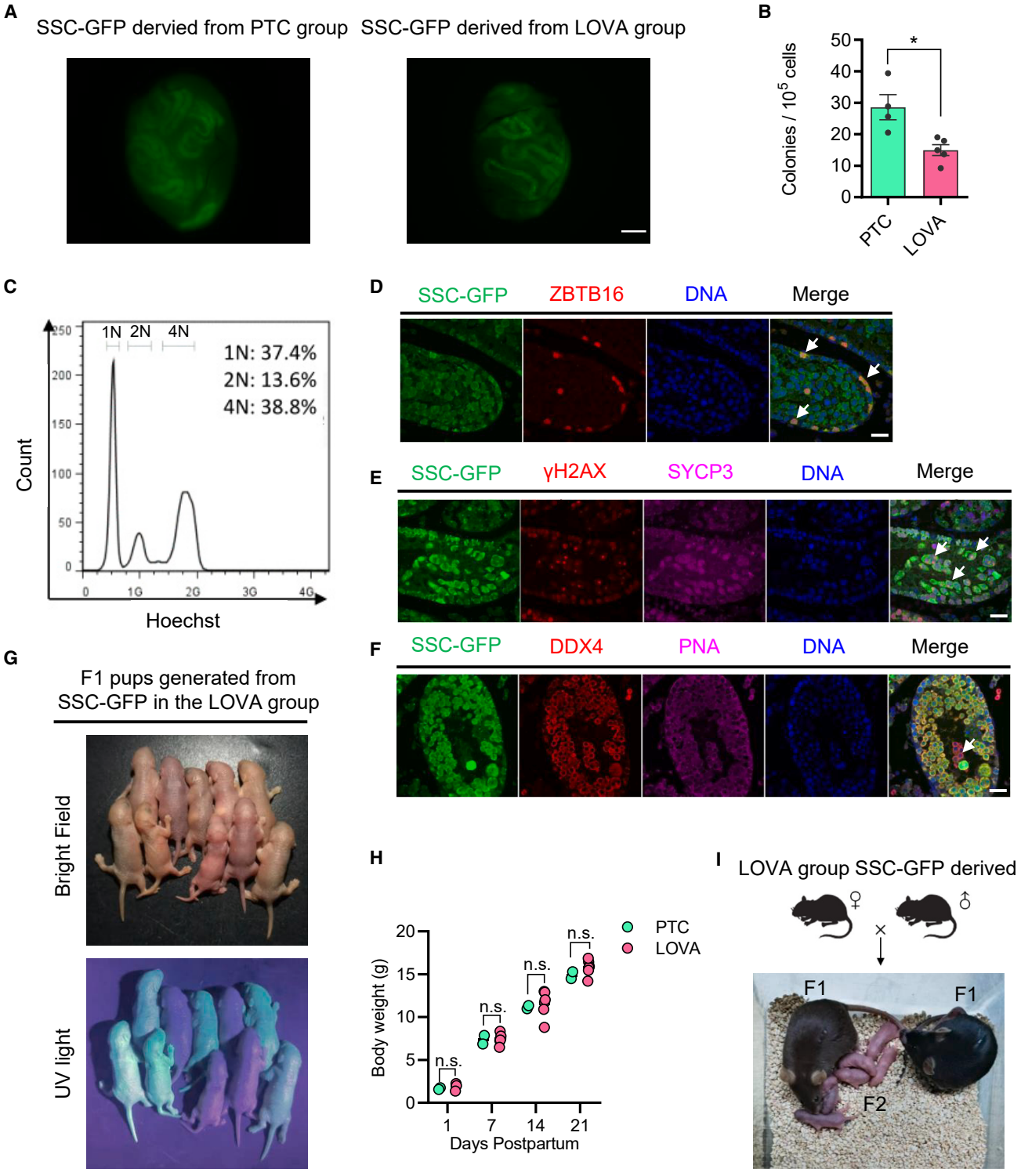

Figure 2. LOVA maintains the function of mSSCs *in vitro* in the absence of GDNF

(A) Cell colonization in the recipient testes. The SSC-GFP cells derived form PTC or LOVA group were transplanted into 5–10 days post partum recipient mice with fetal busulfan pretreatment and then were detected under a fluorescence microscope after 2 months of transplantation. GFP-labeled mSSCs cultured in each group for 60 days were used to conduct the transplantation assay. Scale bar, 500 μm.

(legend continued on next page)

supporting SSC clone formation, and the result showed that 5 μM was the best (Figure S1C).

To prove the direct modulation of LOVA on SSCs, we have interrupted the LOVA regulated pathway through CRISPR-Cas13d-mediated knockdown of LOVA receptor HMG-CoA reductase (HMGCR) (Jiao et al., 2020; Xia et al., 2018) (Figures 1G and 1H). The result showed that knockdown of HMGCR could mimic the promoting effect of LOVA during cells' *in vitro* proliferation in the absence of GDNF (Figure S1D). Consistently, the number of proliferative cultured cells, which was indicated by ID4 and Ki67 double immunostaining, was significantly higher in HMGCR knockdown groups than in the control group, suggesting that LOVA might directly act on mSSCs to promote their proliferation (Figures 1I and 1J). Additionally, we utilized the feeder-free culture method and found that the expression of the markers that related to cell cycles and undifferentiated spermatogonia were significantly higher in the LOVA group than in the NTC group, which supports the conclusion that LOVA acts directly on cultured cells as mentioned above (Figure S1E).

LOVA culture-derived mSSCs could differentiate to functional round spermatids and generate fertile offspring

To assess the differentiation potential of mSSCs cultured in LOVA condition, we conducted SSC transplantation experiments by utilizing GFP-labeled mSSCs (SSC-GFPs). Cells were cultured under LOVA or PTC conditions for 60 days, followed by being transplanted into the testes of recipient pup mice (Shinohara et al., 2001) (Figure 2A). Although the number of colonies derived from the LOVA group was significantly smaller than the PTC group, mSSCs from the LOVA group were capable of colonization in seminiferous tubules (Figure 2B). Two months later, the chromosome ploidy analysis of GFP^+ cells from these seminiferous tubules showed that the cell composition included haploid, diploid, and tetraploid cells, suggesting that the transplanted LOVA-treated mSSCs were capable of colonization for spermatogenesis (Figure 2C). Additionally, the differentiation potential of mSSCs was maintained well after LOVA treatment, with $ZBTB16^+$ undifferentiated spermatogonia, $SYCP3^+\gamma H2AX^+$ spermatocytes, and $DDX4^+PNA^+$ spermatids being detected (Figures 2D–2F). To evaluate the fertility of spermatids derived from exogenous transplanted mSSCs, we performed ROSI (round spermatid injection) and found that embryo developments together with live birth rate were comparable between PTC and LOVA groups (Figures S2A and S2B). Spermatids derived from LOVA conditions generated fertile offspring, whose growth showed no significant differences compared with the PTC group (Figures 2G–2I). Furthermore, after mSSCs from the LOVA group were transplanted into the testes of recipient adult mice, they could colonize in adult testes and differentiate to $ZBTB16^+$ undifferentiated spermatogonia, $DDX4^+SYCP3^+$ spermatocytes, and $DDX4^+PNA^+$ spermatids (Figures S2C–S2F). In summary, mSSCs derived from the LOVA group were capable of colonization in testes from both pup and adult recipient mice. Notably, mSSCs derived from the LOVA group could further reconstitute spermatogenesis to yield fertile spermatids in the testes of pup recipient mice, indicating that LOVA ensured the normal function of mSSCs.

LOVA acts on mSSCs through multiple molecular regulations

To know how LOVA supports the proliferation of mSSCs while maintaining its proper differentiation potential, bulk RNA sequencing (RNA-seq) was performed on cell samples from PTC, LOVA, and NTC groups. Further analysis found that a total of 68 differentially expressed genes (DEGs) (cutoff: top 200 DEGs with $p < 0.05$) were identified between PTC and LOVA groups, in which 56 genes were down-regulated and 12 genes were up-regulated (Figure 3A). Notably, the down-regulated genes were mainly associated with inflammatory response and granulocyte chemotaxis, suggesting that both LOVA and GDNF might be involved in the anti-inflammatory regulation of mSSCs (Figure 3B). To test this hypothesis, cytokine array analysis was performed to evaluate the anti-inflammatory effects in

(B) The statistics of colonized colonies formed by transplantation assay in (A). Error bars indicate mean ± SEM from four independent experiments. $^*p \leq 0.05$.

(C) Flow cytometry analysis of cell karyotype of recipient's seminiferous tubules from the LOVA group. Cells were obtained by enzymatic digestion and then labeled with Hoechst. The karyotypes of GFP^+ cells were detected to contain haploid, diploid, and tetraploid, indicating that the transplanted mSSCs could accomplish the spermatogenesis process.

(D–F) Immunofluorescent staining of colonized exogenous SSC-GFPs in recipient testis section. ZBTB16 (D), SYCP3 and γH2AX (E), and PNA (F) were labeled as markers of undifferentiated spermatogonia, spermatocytes, and spermatids, respectively. Scale bars, 50 μm.

(G) The F1 offspring derived from spermatids that were generated from SSC-GFPs of the LOVA group.

(H) Growth weight analysis of F1 offspring derived from spermatids that were generated from SSC-GFPs from the PTC or LOVA group, respectively.

(I) The F2 offspring derived from F1 offspring in (H).

See also Figure S2.

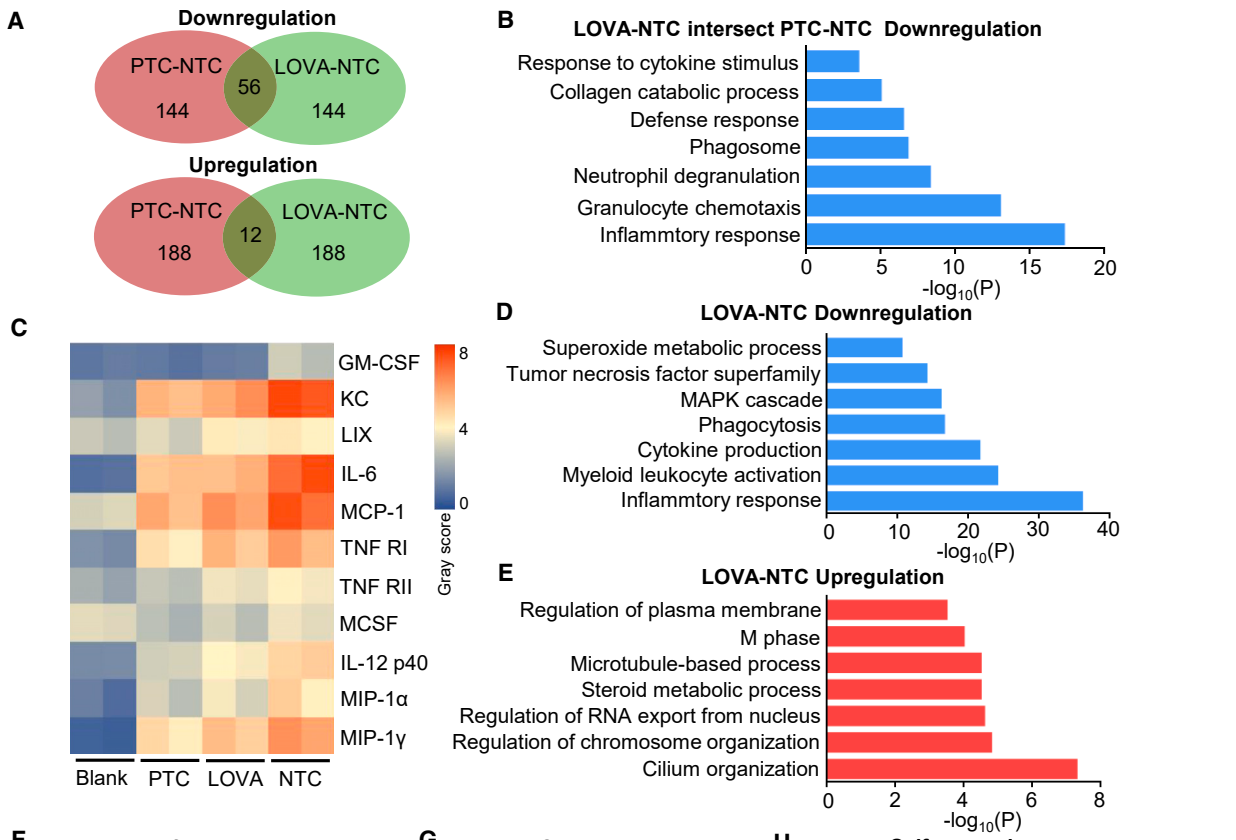

(legend on next page)

these 3 groups. We found that the treatment of mSSCs by either LOVA or PTC could significantly decrease the secretion of cytokines, such as granulocyte-macrophage colony-stimulating factor (GM-CSF), chemokine (C-X-C motif) ligand 1 (CXCL1, a.k.a. KC), C-X-C motif ligand 5 (CXCL5, a.k.a. LIX), interleukin-6 (IL-6), MCP-1, tumor necrosis factor receptor superfamily member 1a (Tnfrsf1a, TNF-RI), TNF RII, IL-12 p40/p70, chemokine (C-C motif) ligand 3 (CCL3, a.k.a. MIP-1α), and C-C motif ligand 9 (CCL9, a.k.a. MIP-1γ) (Figures 3C and S3A). DEG analysis between LOVA and NTC also found that genes down-regulated in LOVA treatment were associated with inflammatory response and cytokine production, while genes in LOVA that regulated cytoskeleton, chromosome organization, and M phase were up-regulated (Figures 3D and 3E). And the representative genes related to inflammation were significantly down-regulated in LOVA, whereas those involved in cell cycles and self-renewal were markedly up-regulated (Figures 3F–3H). Consistent with this finding, we observed a decrease of complement C3 signals in either the LOVA or PTC group compared with the NTC group (Figures 3I and S3B). Based on the RNA-seq results and the fact that complement C3 mediates activation of cell apoptosis (Alexander et al., 2005; Jha et al., 2011; Rensen et al., 2009), it was most likely that apoptosis was more severe in the NTC group. Immunostaining results showed that the signal of cleaved caspase-3 was higher in NTC than that of either the LOVA or PTC group (Figures 3J and S3C), which was further supported by qPCR results, in which the expression of proapoptotic genes was down-regulated (e.g., *Bax* and *Fadd*), whereas the anti-apoptotic gene was up-regulated (e.g., Bcl2), in the LOVA group compared with the NTC group (Figure S3D) (Ge et al., 2019; Mao et al., 2021). Together, LOVA was essential for the alleviation of inflammation and apoptosis in mSSCs.

Statins inhibit apoptosis potentially through mevalonate cascades to support mSSC self-renewal

Statins have a great lipid-lowering function by blocking the mevalonate metabolic pathway through competitive inhibition of HMGCR (Jiao et al., 2020; Xia et al., 2018) (Figure 4A). Increasing evidence shows that statins could exert anti-inflammatory and anti-apoptotic functions both *in vitro* and *in vivo* (Parihar et al., 2019; Tripathi et al., 2018; Xia et al., 2018). To confirm if statins exert function through the mevalonate pathway, functional studies were performed accordingly. We found that the addition of three intermediate metabolites of the mevalonate pathway, including geranyl pyrophosphate (GPP), fagini pyrophosphate (FPP), and squalene, can abolish the anti-apoptotic effect of LOVA in mSSCs. Of note, the addition of FPP led to the highest level of cell apoptosis (Figures 4B and 4C). These results suggest that LOVA played an anti-apoptotic role in mSSCs by inhibiting the downstream metabolites of the mevalonate pathway.

To further test if other statins also exert anti-inflammatory and anti-apoptotic effects on mSSCs, eight commercially available statins were then evaluated. Our results showed that all the tested statins could promote the proliferation of mSSCs compared with the control group (Figure 4D). Among these statins, the effect of fluvastatin (FLUVA) not only had an effect on promoting the proliferation of undifferentiated spermatogonia for further verification but also decreased the levels of complement 3 and cleaved caspase-3 (Figures 4E and 4F). Consistent with this, the expressions of *Apoe* and *Cd68* have markedly decreased in mSSCs derived from the FLUVA group. In contrast, the expression of *Etv5*, a typical marker of mSSCs, was significantly increased (Figures 4G and 4H). In addition, cell numbers that were double stained with ID4 and Ki67, classical markers of proliferative mSSCs, were significantly higher in the FLUVA group than in the NTC group (Figures 4I and 4J), raising the possibility that other statins exert similar effects on cultured cells. These results indicate that statins might inhibit apoptosis through the mevalonate pathway to support the proliferation of mSSCs.

LOVA promotes the proliferation of testicular undifferentiated spermatogonia and reduces their apoptosis under spermatogenesis defective conditions

To know if the LOVA could promote the proliferation of mSSCs *in vivo*, intraperitoneal (i.p.) injection of LOVA was

Figure 3. LOVA promotes mSSC self-renewal as well as inhibits inflammation and apoptosis

(A) Venn diagram showing the intersection of differentially expressed genes between different comparisons.

(B) GO analysis of significantly down-regulated genes in both LOVA vs. NTC and PTC vs. NTC.

(C) Heatmap of cytokine array analysis.

(D) GO analysis of LOVA down-regulated genes compared with NTC.

(E) GO analysis of LOVA up-regulated genes compared with NTC.

(F–H) qPCR analysis of the relative expression level of representative genes regarding inflammation (F), cell cycle (G), and self-renewal (H). Error bars indicate mean ± SEM from three independent experiments, ***$p \leq 0.001$, ****$p \leq 0.0001$.

(I and J) Immunofluorescent staining of complement 3 (I) or cleaved caspase-3 (J) in ZBTB16-labeled undifferentiated spermatogonia clones cultured in 3 different groups. Scale bars, 50 μm.

See also Figure S3.

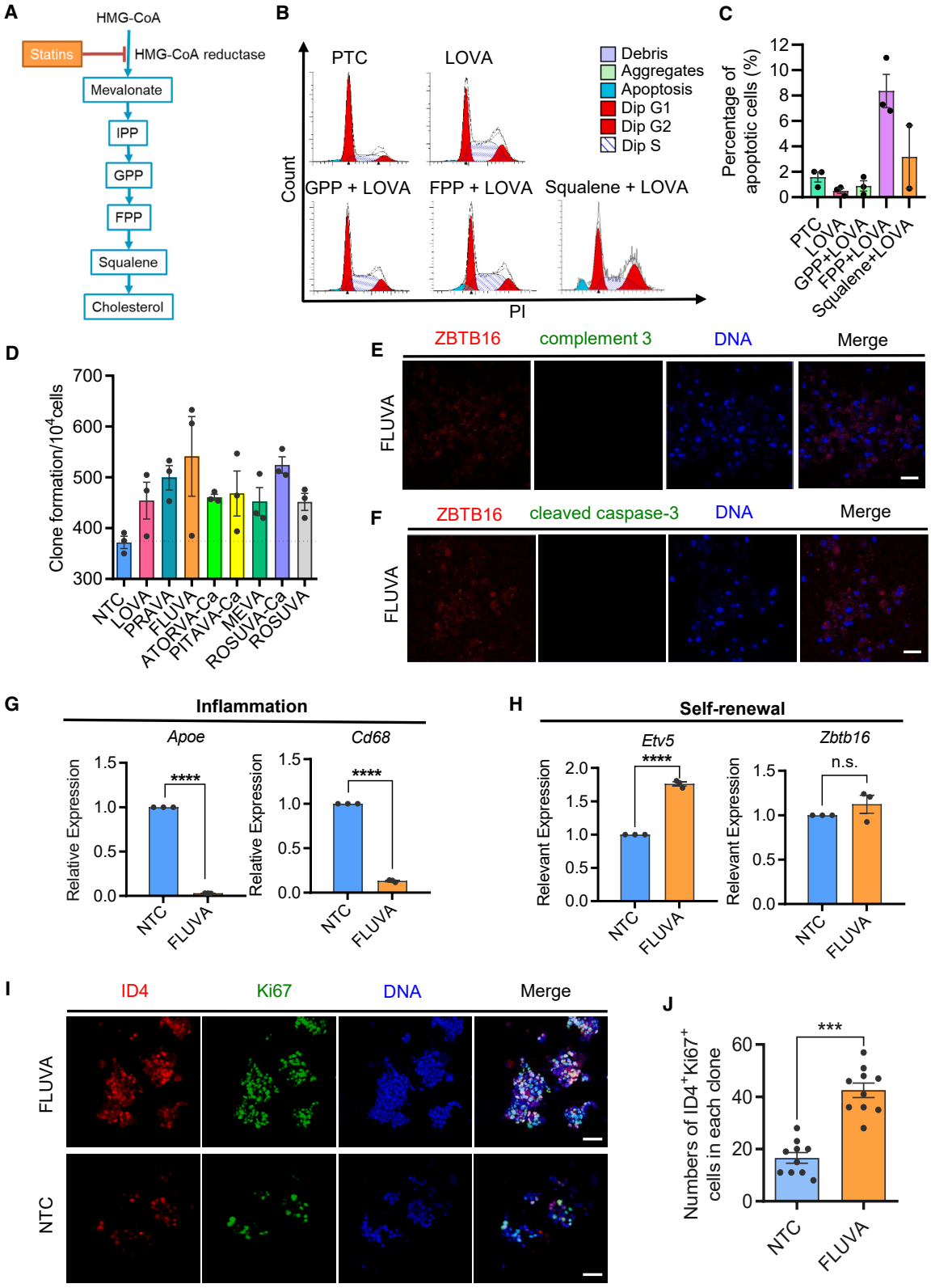

(legend on next page)

performed on mice daily with dosages of 1, 5, and 10 mg/kg for 5 days, with the mice injected with isotypic solvent as the control. After 5 days, the testes were collected to detect the proliferation of undifferentiated spermatogonia by immunostaining (Figure S4A). We found that the signal of Ki67 in undifferentiated spermatogonia was increased in LOVA-treated mice compared with the control, indicating that LOVA could promote the proliferation of undifferentiated spermatogonia *in vivo* (Figures S4B–S4D).

We then injected busulfan-treated mice with LOVA to evaluate if LOVA could induce the proliferation of undifferentiated spermatogonia in the spermatogenesis defective condition (Figure 5A). Five days later, the LOVA group exhibited a significant increase of ZBTB16^{+}Ki67^{+} proliferative undifferentiated spermatogonia. The increase of ZBTB16^{+}Ki67^{+} spermatogonia in the LOVA-treated group could still be observed after 10 days, when the number of undifferentiated spermatogonia in the control group gradually recovered (Figures 5B, 5C, and S4E).

To confirm if LOVA could protect the *in vivo* undifferentiated spermatogonia from apoptosis during the process of the busulfan treatment, we administrated LOVA simultaneously with busulfan treatment (Figure 5D). We found that LOVA could significantly decrease apoptosis in testicular undifferentiated spermatogonia (Figures 5E–5G). These results demonstrated that LOVA could promote the proliferation of undifferentiated spermatogonia under both normal and spermatogenesis defective conditions and prevent the testicular undifferentiated spermatogonia from apoptosis.

LOVA promotes the proliferation of primate undifferentiated spermatogonia of *in vitro* organ culture

To test if LOVA could promote the proliferation of primate spermatogonia, we established a temporary primate testicular culture system (Figure 6A) in which human and cynomolgus monkey spermatogonia could be maintained well on the basement membrane of a seminiferous tubule for more than 30 days. LOVA was added to the culture medium to evaluate its effects. After treatment for 14 days, cynomolgus monkey or human samples were collected to evaluate the number of germ cells including undifferentiated spermatogonia (von Kopylow et al., 2010; Wu et al., 2009). We found that the number of either prepuberty or adult monkey undifferentiated spermatogonia in the lumen was higher in the LOVA-treated group than in the control group, especially adult monkeys, which had a significant increase (Figures 6B–6E). Similarly, the number of human undifferentiated spermatogonia in the lumen was also significantly higher in the LOVA-treated group than in the control group (Figures 6F and 6G). These data suggest that LOVA significantly promoted the proliferation of primate undifferentiated spermatogonia.

DISCUSSION

SSCs that are capable of repopulating spermatogenesis have ceased due to the side effect of chemotherapy to the SSC niche, including GDNF reduction, inflammation, and apoptosis (Harman and Richburg, 2014; Morimoto et al., 2021; Qian et al., 2020; Zhang et al., 2013). Apart from the key regulator of SSC self-renewal, GDNF also involves anti-inflammation and anti-apoptosis, which made it essential for SSC propagation *in vivo* and *in vitro* (Gao et al., 2014; Kanatsu-Shinohara et al., 2003; Kubota et al., 2004; Masaki et al., 2018; Meng et al., 2000; Sharma and Braun, 2018; Tadokoro et al., 2002; Tan et al., 2020; Wang et al., 2019). Therefore, we set up a drug screening system to identify potential candidates that promote mSSC self-renewal independent of GDNF, which may provide a hint for SSC recovery in defected testis. As a result, we identified LOVA, which promotes mSSC self-renewal, exhibits typical SSC morphologies, and expresses mSSC key markers. Importantly, mSSCs derived from the LOVA group

Figure 4. Statins play an anti-apoptotic role by regulating the mevalonate pathway

(A) Schematic diagram of statin-dependent regulation of mevalonate metabolism.

(B) Fluorescence-activated cell sorting (FACS) analysis of cell apoptosis and cell-cycle distribution.

(C) Statistic histogram of apoptosis proportion for each treatment group. Error bars indicate mean ± SEM from three independent experiments.

(D) mSSC clone formation analysis after treatment with 8 kinds of statins. Error bars indicate mean ± SEM from three independent experiments.

(E and F) Immunofluorescent staining of undifferentiated spermatogonia marker (ZBTB16) and complement 3 (E) or cleaved caspase-3 (F) in mSSC clones cultured in the fluvastatin (FLUVA) group. Scale bars, 50 μm.

(G and H) qPCR analysis of the relative expression level of representative genes regarding inflammation (G) and self-renewal (H). Error bars indicate mean ± SEM from three independent experiments. ****$p \leq 0.0001$, ns, non-significant.

(I) Immunofluorescent staining of ID4^{+} Ki67^{+} cells in mSSC clones cultured in NTC or FLUVA group. Scale bars, 50 μm.

(J) Statistic histogram of ID4 and Ki67 double-positive cells from FLUVA or NTC group from ten independent experiments. Error bars indicate mean ± SEM, ***$p \leq 0.001$.

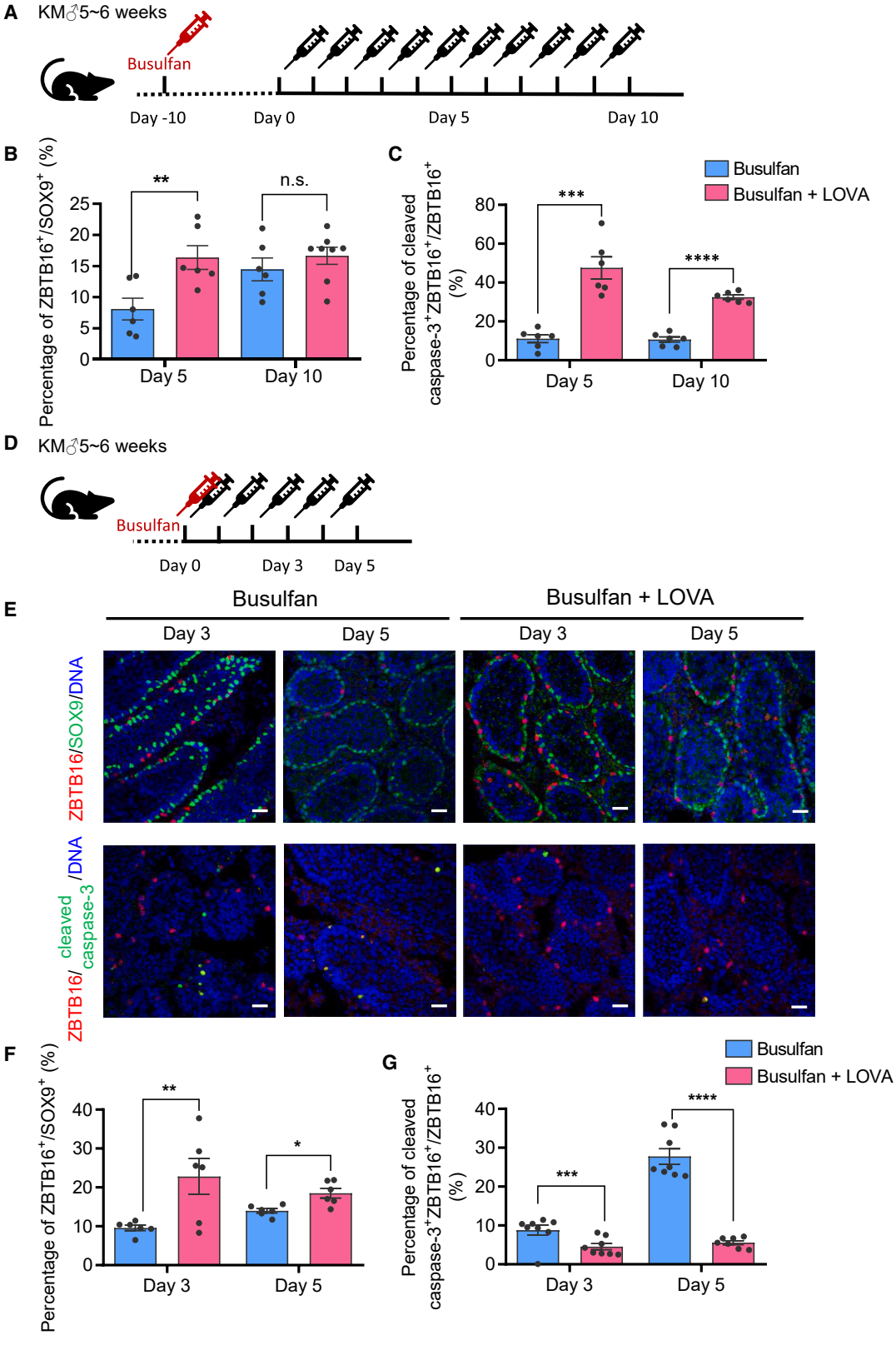

(legend on next page)

were capable for spermatogenesis that generate fertile offspring after being transplanted into the testes of recipient mice, indicating that LOVA ensures normal mSSC functions while faithfully promoting mSSC self-renewal. Further mechanism analysis suggested effects of LOVA on SSCs through multiple layers, including promotion of self-renewal and cell cycle as well as inhibition of inflammation and apoptosis, which might partially substitute and fulfill the role of GDNF in mSSC proliferation (Gao et al., 2014; Kubota et al., 2004; Masaki et al., 2018; Meng et al., 2000; Sharma and Braun, 2018; Tadokoro et al., 2002; Wang et al., 2019), as statins inhibit HMGCR, the rate-limiting enzyme of the L-mevalonate pathway, thereby preventing the formation of downstream metabolites (Assmus et al., 2003; Zeiser, 2018; Zeiser et al., 2009). Hence, we tested and found that the addition of downstream metabolites such as GPP, FPP, and squalene were capable of abolishing LOVA-mediated apoptosis prevention to mSSCs, suggesting that inhibitory effects of LOVA are dependent on HMGCR. Likewise, other statins that share the same target for HMGCR inhibition also demonstrate similar effects, indicating that the effects of LOVA on mSSCs could be generalized to various statins, which expands our knowledge that HMGCR inhibitors could control cell proliferation (Assmus et al., 2003; Chen et al., 2008; Mills et al., 2019). Intriguingly, the mechanisms of how the downstream metabolites of HMGCR are involved in mSSC proliferation remain elusive and require further study.

Prior studies have suggested that the effects of statins may be diverse to different types of stem cells (Assmus et al., 2003; Gauthaman et al., 2009; Kupcsik et al., 2009; Xu et al., 2009, 2013). Of note, statins could promote self-renewal and then benefit further differentiation for normal embryonic stem cells (ESCs) but inhibit the growth of variant ESCs (Gauthaman et al., 2009). In order to investigate the effects of LOVA in the impaired mSSC niche, we injected busulfan into mice to simulate chemotherapy, followed by LOVA treatments. Our finding reveals that LOVA could not only promote the recovery of undifferentiated spermatogonia but could also protect undifferentiated spermatogonia during chemotherapy treatment. Due to its role in anti-apoptosis, we speculated that LOVA alleviated the damage to mSSC niche by anti-inflammation, thereby creating a microenvironment that is suitable for mSSC survival and self-renewal, which partially substitute GDNF for its anti-inflammatory and protective efficacy during gonadotoxic therapies (Morimoto et al., 2021). Of note, statin medication has its advantages over GDNF in clinical applications for the following reasons. Firstly, GDNF is a neurotrophin that plays an important role in the nervous system, in renal morphogenesis, and in spermatogenesis, which has complicated its clinical use (Ibanez and Andressoo, 2017; Jain, 2009; Lin et al., 1993; Meng et al., 2000). Additionally, increasing evidence shows that GDNF might be involved in tumor progression. These findings are also supported by the fact that overexpression of GDNF could result in the generation of the seminoma-like tumor, thereby eliciting concerns about its safety in clinical use (Airaksinen and Saarma, 2002; Meng et al., 2000). In contrast, the safety of statin medication has been validated, making it more suitable for potential use in treating male infertility (Athyros et al., 2010; Gu et al., 2019; Jiang et al., 2018; Yan et al., 2013).

In the past years, numerous studies have been carried out to explore the efficient utility of gamete cells by increasing the proliferation and differentiation of spermatogonia in primates including human beings (Fayomi et al., 2019; Tan et al., 2020). However, there are still several bottlenecks that limit the development of this field, such as an *in vitro* spermatogonial cell culture system for primates. Therefore,

Figure 5. LOVA could promote the proliferation of undifferentiated spermatogonia and protect undifferentiated spermatogonias from apoptosis damage *in vivo*

(A) Schematic outline of LOVA injection after 10 days of busulfan treatment in order to simulate reparation after chemotherapy.

(B) Histogram calculation of the proportion of undifferentiated spermatogonia (ZBTB16$^+$ cells) compared with Sertoli cells (SOX9$^+$ cells) in (A) from six independent experiments. Error bars indicate mean ± SEM, $^{**}p \leq 0.01$, ns, non-significant.

(C) Histogram calculation of the proportion of cleaved caspase-3$^+$ ZBTB16$^+$-double labeled apoptotic undifferentiated spermatogonia compared with ZBTB16$^+$-labeled undifferentiated spermatogonia in (A) from six independent experiments. Error bars indicate mean ± SEM, $^{***}p \leq 0.001$, $^{****}p \leq 0.0001$.

(D) Schematic outline of mouse treated by busulfan simultaneously with LOVA injection in order to estimate the prevention of chemotherapy injury.

(E) Immunofluorescent staining of undifferentiated spermatogonia marker (ZBTB16) and Sertoli cell marker (SOX9) or apoptotic cell markers (cleaved caspase-3) in mouse testis under the treatment of busulfan with or without LOVA injection. Scale bars, 50 μm.

(F) Histogram calculation of the proportion of undifferentiated spermatogonia (ZBTB16$^+$ cells) compared with Sertoli cells (SOX9$^+$ cells) in (E) from six independent experiments. Error bars indicate mean ± SEM, $^{*}p \leq 0.05$, $^{**}p \leq 0.01$.

(G) Histogram calculation of the proportion of cleaved caspase-3$^+$ZBTB16$^+$-labeled apoptotic undifferentiated spermatogonia compared with total ZBTB16$^+$-labeled undifferentiated spermatogonia in (E) from six independent experiments. Error bars indicate mean ± SEM, $^{***}p \leq 0.001$, $^{****}p \leq 0.0001$.

See also Figure S4.

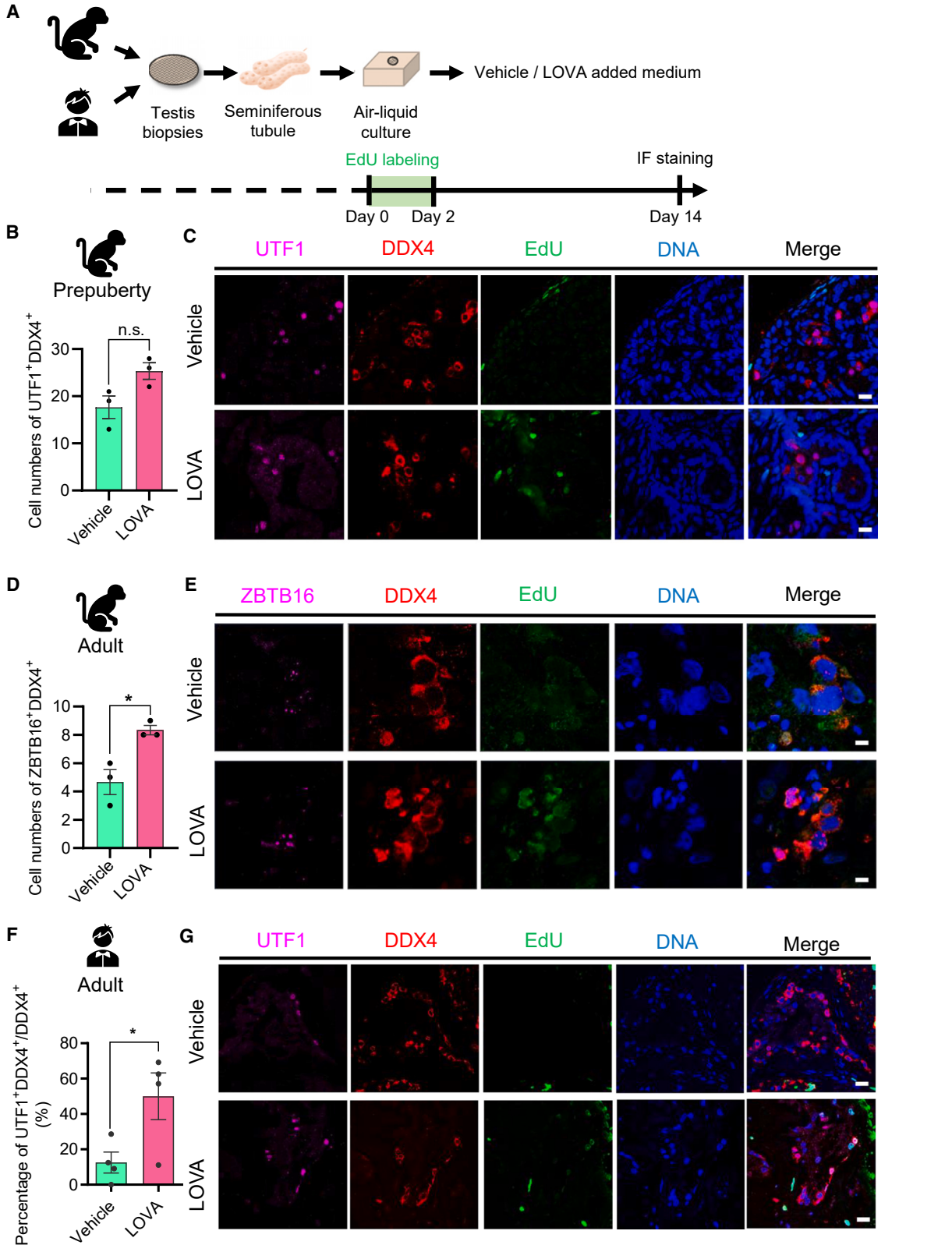

(legend on next page)

based on the study of a LOVA culture system in rodent, we then made a preliminary attempt by applying LOVA in the testicular organ culture, which was derived from monkeys and humans with normal spermatogenesis. Immunofluorescence analysis indicated that LOVA improves the maintenance of germ cells and undifferentiated spermatogonia to varying degrees, with significant elevation of undifferentiated spermatogonia in human samples, suggesting the conserved role of LOVA acting on spermatogonia. Notably, statins showed pleiotropic effects in cancer therapy including great suppression on tumor growth, induction of apoptosis in specific cancer cell types, and chemo-sensitizing effects (Ahmadi et al., 2020; Clendening and Penn, 2012; Gopalan et al., 2013; Likus et al., 2016; Sadaria et al., 2011; Yin et al., 2018). Given that statins promote undifferentiated spermatogonia proliferation in the defected testicular niche, we proposed statins hold promise for future clinical application of repopulating spermatogenesis.

EXPERIMENTAL PROCEDURES

Resource availability

Corresponding author

Further information and requests for resources and reagents should be directed to and will be fulfilled by the corresponding author, Xiao-Yang Zhao (zhaoxiaoyang@smu.edu.cn).

Materials availability

Not applicable.

Data and code availability

The accession number for raw data and processed data in this article is GEO: GSE182897.

Human seminiferous tubule *in vitro* culture

Biopsies of human testicular tissue samples were obtained and washed twice with PBS. The sample was dissociated into 2 mm pieces by tweezer, put on 1% agarose gel, and then cultured with SSC culture medium. In detail, StemPro-34 SFM (Invitrogen) with its supplement and 1% knockout serum replacement (Thermo Fisher Scientific, A3181502) were added. The medium were supplied with 0.1 mM NEAA; 1 mM sodium pyruvate; 2 mM GlutaMAX; 100 U/mL penicillin; 0.1 mg/mL streptomycin; 50 μM β-mercaptoethanol; 1 μL/mL DL-lactic acid; 1 × minimal essential medium (MEM) vitamin solution; 10 μg/mL biotin; 100 μM ascorbic acid; 60 ng/mL progesterone; 30 ng/mL β-estradiol; 6 mg/mL glucose; 5 mg/mL BSA; 1% N2 supplement; 20 ng/mL recombinant human GDNF (R&D Systems, 212-GD); and 10 ng/mL recombinant human FGF2 (R&D Systems, 233-FB). 5 μM LOVA (TargetMol, T1207) or DMSO solvent was added as necessary. The sample was incubated at 34°C, and the medium was changed every other day.

Cytokine array

Culture media of different SSC treatment conditions were collected from days 12 to 18, and all media were concentrated proportionally to 1 m using a prechilled centrifugal. Forty cytokines were detected according to the manufacturer's instructions of Mouse Inflammation Antibody Array Membrane (Abcam, ab133999). Chemiluminescence imaging of all spots in the array membrane was performed using blot documentation systems, and the signal density of each spot was measured by densitometric analysis using ImageJ. For background subtraction and normalization, the raw numerical data of each spot were subtracted from the mean of negative control spots then normalized based on the mean of positive control spots.

SUPPLEMENTAL INFORMATION

Supplemental information can be found online at https://doi.org/10.1016/j.stemcr.2023.02.011.

AUTHOR CONTRIBUTIONS

X.-Y.Z., F.L., and K.M. conceptualized this project and supervised the overall experiments. C.L., Z.Y., and C.W. established the SSC cell line and performed the small-molecule screening and all cell culture relevant work. Z.Y. and S.R. performed SSC transplantation and ROSI. L.M. and W.W. raised the mice and performed *in vivo* injections. L.M. and D.C. performed all molecule-relevant work. X.S. and F.L. performed bioinformatics analysis. Y.-t.Z. operated human testicular biopsies. G.C. and S.W revised the data and proofread the

Figure 6. LOVA promotes the proliferation of *in-vitro*-cultured primate undifferentiated spermatogonia

(A) Schematic outline of primate seminiferous tubule culture condition *in vitro*.

(B) Histogram calculation of the germ cell number in seminiferous tubules from three independent experiments. Error bars indicate mean ± SEM, ns, non-significant.

(C) Immunofluorescent staining of undifferentiated spermatogonia marker (UTF1), germ cell marker (DDX4), and EdU expression in prepuberty seminiferous tubule cultured tissue. Scale bars, 20 μm.

(D) Histogram calculation of the germ cell number in seminiferous tubules from three independent experiments. Error bars indicate mean ± SEM, *p ≤ 0.05.

(E) Immunofluorescent staining of undifferentiated spermatogonia marker (ZBTB16), germ cell marker (DDX4), and EdU expression in seminiferous tubule cultured tissue. Scale bars, 10 μm.

(F) Histogram calculation of the proportion of undifferentiated spermatogonia in seminiferous tubules from four independent experiments. Error bars indicate mean ± SEM, *p ≤ 0.05.

(G) Immunofluorescent staining of undifferentiated spermatogonia marker (UTF1), germ cell marker (DDX4), and EdU expression in seminiferous tubule cultured tissue. Scale bars, 20 μm.

manuscript. X.-Y.Z., F.L., K.M., C.L., and Z.Y. wrote the manuscript with the help from all the authors.

ACKNOWLEDGMENTS

We are grateful to Dr. Zhao Yang from Peking University for providing us with the small-molecule compound library. This work was supported by grants from the National Key Research and Development Program of China (2022YFA0806301 to F.L. and 2022YFA0806303, 2022YFC2702603, and 2017YFA0105001 to X.-Y.Z.); the National Natural Science Foundation of China (82071711 and U22A20278 to X.-Y.Z., 31700676 to F.L., 31970787 and 32170869 to G.C., and 3210060082 to C.L.); Guangdong Basic and Applied Basic Research Foundation (2020A1515010877 to C.L.); Guangdong Natural Science Foundation (2019A1515010446 to G.C.); the Natural Science Foundation of Shenzhen (JCYJ20210324120212033 and JCYJ20180305163311448 to G.C.); and China Postdoctoral Science Foundation (2019M652954 to C.L.).

CONFLICT OF INTERESTS

The authors declare no competing interests.

Received: September 15, 2021
Revised: February 24, 2023
Accepted: February 24, 2023
Published: April 11, 2023

REFERENCES

Ahmadi, M., Amiri, S., Pecic, S., Machaj, F., Rosik, J., Łos, M.J., Alizadeh, J., Mahdian, R., da Silva Rosa, S.C., Schaafsma, D., et al. (2020). Pleiotropic effects of statins: a focus on cancer. Biochim. Biophys. Acta. Mol. Basis Dis. *1866*, 165968.

Airaksinen, M.S., and Saarma, M. (2002). The GDNF family: signalling, biological functions and therapeutic value. Nat. Rev. Neurosci. *3*, 383–394.

Alexander, J.J., Jacob, A., Bao, L., Macdonald, R.L., and Quigg, R.J. (2005). Complement-dependent apoptosis and inflammatory gene changes in murine lupus cerebritis. J. Immunol. *175*, 8312–8319.

Allen, C.M., Lopes, F., Mitchell, R.T., and Spears, N. (2018). How does chemotherapy treatment damage the prepubertal testis? Reproduction *156*, R209–R233.

Assmus, B., Urbich, C., Aicher, A., Hofmann, W.K., Haendeler, J., Rössig, L., Spyridopoulos, I., Zeiher, A.M., and Dimmeler, S. (2003). HMG-CoA reductase inhibitors reduce senescence and increase proliferation of endothelial progenitor cells via regulation of cell cycle regulatory genes. Circ. Res. *92*, 1049–1055.

Athyros, V.G., Tziomalos, K., Gossios, T.D., Griva, T., Anagnostis, P., Kargiotis, K., Pagourelias, E.D., Theocharidou, E., Karagiannis, A., and Mikhailidis, D.P.; GREACE Study Collaborative Group (2010). Safety and efficacy of long-term statin treatment for cardiovascular events in patients with coronary heart disease and abnormal liver tests in the Greek Atorvastatin and Coronary Heart Disease Evaluation (GREACE) Study: a post-hoc analysis. Lancet *376*, 1916–1922.

Benavides-Garcia, R., Joachim, R., Pina, N.A., Mutoji, K.N., Reilly, M.A., and Hermann, B.P. (2015). Granulocyte colony-stimulating factor prevents loss of spermatogenesis after sterilizing busulfan chemotherapy. Fertil. Steril. *103*, 270–280.e8.

Brilhante, O., Okada, F.K., Sasso-Cerri, E., Stumpp, T., and Miraglia, S.M. (2012). Late morfofunctional alterations of the Sertoli cell caused by doxorubicin administered to prepubertal rats. Reprod. Biol. Endocrinol. *10*, 79.

Chan, F., Oatley, M.J., Kaucher, A.V., Yang, Q.E., Bieberich, C.J., Shashikant, C.S., and Oatley, J.M. (2014). Functional and molecular features of the Id4+ germline stem cell population in mouse testes. Genes DevGenes Dev. *28*, 1351–1362.

Chen, J., Zacharek, A., Li, A., Cui, X., Roberts, C., Lu, M., and Chopp, M. (2008). Atorvastatin promotes presenilin-1 expression and Notch1 activity and increases neural progenitor cell proliferation after stroke. Stroke *39*, 220–226.

Chen, L.Y., Willis, W.D., and Eddy, E.M. (2016). Targeting the Gdnf Gene in peritubular myoid cells disrupts undifferentiated spermatogonial cell development. ProcProc. Natl. Acad. Sci. USA *113*, 1829–1834.

Chen, S.R., and Liu, Y.X. (2015). Regulation of spermatogonial stem cell self-renewal and spermatocyte meiosis by Sertoli cell signaling. Reproduction *149*, R159–R167.

Chen, Z., Liu, M., Hu, J.H., Gao, Y., Deng, C., and Jiang, M.H. (2021). Substance P restores spermatogenesis in busulfan-treated mice: a new strategy for male infertility therapy. Biomed. Pharmacother. *133*, 110868.

Clendening, J.W., and Penn, L.Z. (2012). Targeting tumor cell metabolism with statins. Oncogene *31*, 4967–4978.

Clermont, Y. (1972). Kinetics of spermatogenesis in mammals: seminiferous epithelium cycle and spermatogonial renewal. Physiol. Rev. *52*, 198–236.

de Rooij, D.G. (2017). The nature and dynamics of spermatogonial stem cells. Development *144*, 3022–3030.

Delessard, M., Saulnier, J., Rives, A., Dumont, L., Rondanino, C., and Rives, N. (2020). Exposure to chemotherapy during childhood or adulthood and consequences on spermatogenesis and male fertility. Int. J. Mol. Sci. *21*, 1454.

Fayomi, A.P., and Orwig, K.E. (2018). Spermatogonial stem cells and spermatogenesis in mice, monkeys and men. Stem Cell Res. *29*, 207–214.

Fayomi, A.P., Peters, K., Sukhwani, M., Valli-Pulaski, H., Shetty, G., Meistrich, M.L., Houser, L., Robertson, N., Roberts, V., Ramsey, C., et al. (2019). Autologous grafting of cryopreserved prepubertal rhesus testis produces sperm and offspring. Science *363*, 1314–1319.

Gao, X., Du, J., Fan, G., Yang, C., Deng, L., and Yuan, Q. (2014). Adenoviral-mediated GDNF protects bone marrow mesenchymal stem cells against apoptosis induced by hydrogen peroxide. Biomed. Mater. Eng. *24*, 2169–2176.

Gauthaman, K., Manasi, N., and Bongso, A. (2009). Statins inhibit the growth of variant human embryonic stem cells and cancer cells in vitro but not normal human embryonic stem cells. Br. J. Pharmacol. *157*, 962–973.

Ge, L., Zhang, X., Hu, S., Song, Y., Kong, J., Zhang, B., and Yang, X. (2019). H19 suppresses the growth of hepatoblastoma cells by

promoting their apoptosis via the signaling pathways of miR-675/FADD and miR-138/PTK2. J. Cell. Biochem. *120*, 5218–5231.

Gopalan, A., Yu, W., Sanders, B.G., and Kline, K. (2013). Eliminating drug resistant breast cancer stem-like cells with combination of simvastatin and gamma-tocotrienol. Cancer Lett. *328*, 285–296.

Gu, Y., Yang, X., Liang, H., and Li, D. (2019). Comprehensive evaluation of effects and safety of statin on the progression of liver cirrhosis: a systematic review and meta-analysis. BMC Gastroenterol. *19*, 231.

Harman, J.G., and Richburg, J.H. (2014). Cisplatin-induced alterations in the functional spermatogonial stem cell pool and niche in C57/BL/6J mice following a clinically relevant multi-cycle exposure. Toxicol. Lett. *227*, 99–112.

Ibanez, C.F., and Andressoo, J.O. (2017). Biology of GDNF and its receptors - relevance for disorders of the central nervous system. Neurobiol. Dis. *97*, 80–89.

Jain, S. (2009). The many faces of RET dysfunction in kidney. Organogenesis *5*, 177–190.

Jha, P., Banda, H., Tytarenko, R., Bora, P.S., and Bora, N.S. (2011). Complement mediated apoptosis leads to the loss of retinal ganglion cells in animal model of glaucoma. Mol. Immunol. *48*, 2151–2158.

Jiang, R., Zhao, S., Wang, R., Feng, H., Zhang, J., Li, X., Mao, Y., Yuan, X., Fei, Z., Zhao, Y., et al. (2018). Safety and efficacy of atorvastatin for chronic subdural hematoma in Chinese patients: a randomized ClinicalTrial. JAMA Neurol. *75*, 1338–1346.

Jiao, Z., Cai, H., Long, Y., Sirka, O.K., Padmanaban, V., Ewald, A.J., and Devreotes, P.N. (2020). Statin-induced GGPP depletion blocks macropinocytosis and starves cells with oncogenic defects. Proc. Natl. Acad. Sci. USA *117*, 4158–4168.

Kanatsu-Shinohara, M., Inoue, K., Ogonuki, N., Morimoto, H., Ogura, A., and Shinohara, T. (2011). Serum- and feeder-free culture of mouse germline stem cells. Biol. Reprod. *84*, 97–105.

Kanatsu-Shinohara, M., Miki, H., Inoue, K., Ogonuki, N., Toyokuni, S., Ogura, A., and Shinohara, T. (2005). Long-term culture of mouse male germline stem cells under serum-or feeder-free conditions. Biol. Reprod. *72*, 985–991.

Kanatsu-Shinohara, M., Ogonuki, N., Inoue, K., Miki, H., Ogura, A., Toyokuni, S., and Shinohara, T. (2003). Long-term proliferation in culture and germline transmission of mouse male germline stem cells. Biol. Reprod. *69*, 612–616.

Kotzur, T., Benavides-Garcia, R., Mecklenburg, J., Sanchez, J.R., Reilly, M., and Hermann, B.P. (2017). Granulocyte colony-stimulating factor (G-CSF) promotes spermatogenic regeneration from surviving spermatogonia after high-dose alkylating chemotherapy. Reprod. Biol. Endocrinol. *15*, 7.

Kubota, H., Avarbock, M.R., and Brinster, R.L. (2004). Growth factors essential for self-renewal and expansion of mouse spermatogonial stem cells. ProcProc. Natl. Acad. Sci. USA *101*, 16489–16494.

Kubota, H., and Brinster, R.L. (2018). Spermatogonial stem cells. Biol. Reprod. *99*, 52–74.

Kupcsik, L., Meurya, T., Flury, M., Stoddart, M., and Alini, M. (2009). Statin-induced calcification in human mesenchymal stem cells is cell death related. J. Cell. Mol. Med. *13*, 4465–4473.

Likus, W., Siemianowicz, K., Bienk, K., Pakula, M., Pathak, H., Dutta, C., Wang, Q., Shojaei, S., Assaraf, Y.G., Ghavami, S., et al. (2016). Could drugs inhibiting the mevalonate pathway also target cancer stem cells? Drug Resist. Updates *25*, 13–25.

Lin, L.F., Doherty, D.H., Lile, J.D., Bektesh, S., and Collins, F. (1993). GDNF: a glial cell line-derived neurotrophic factor for midbrain dopaminergic neurons. Science *260*, 1130–1132.

Liu, M., Hales, B.F., and Robaire, B. (2014). Effects of four chemotherapeutic agents, bleomycin, etoposide, cisplatin, and cyclophosphamide, on DNA damage and telomeres in a mouse spermatogonial cell line. Biol. Reprod. *90*, 72.

Mao, M.G., Xu, J., Liu, R.T., Ye, L., Wang, R., and Jiang, J.L. (2021). Fas/FasL of pacific cod mediated apoptosis. Dev. Comp. Immunol. *119*, 104022.

Marcon, L., Zhang, X., Hales, B.F., Nagano, M.C., and Robaire, B. (2010). Development of a short-term fluorescence-based assay to assess the toxicity of anticancer drugs on rat stem/progenitor spermatogonia in vitro. Biol. Reprod. *83*, 228–237.

Masaki, K., Sakai, M., Kuroki, S., Jo, J.I., Hoshina, K., Fujimori, Y., Oka, K., Amano, T., Yamanaka, T., Tachibana, M., et al. (2018). FGF2 has distinct molecular functions from GDNF in the mouse germline niche. Stem Cell Rep. *10*, 1782–1792.

Mei, X.X., Wang, J., and Wu, J. (2015). Extrinsic and intrinsic factors controlling spermatogonial stem cell self-renewal and differentiation. Asian J. Androl. *17*, 347–354.

Meistrich, M.L. (1993). Effects of chemotherapy and radiotherapy on spermatogenesis. Eur. Urol. *23*, 136–141. discussion 142.

Meistrich, M.L. (2013). Effects of chemotherapy and radiotherapy on spermatogenesis in humans. Fertil. Steril. *100*, 1180–1186.

Meng, X., Lindahl, M., Hyvönen, M.E., Parvinen, M., de Rooij, D.G., Hess, M.W., Raatikainen-Ahokas, A., Sainio, K., Rauvala, H., Lakso, M., et al. (2000). Regulation of cell fate decision of undifferentiated spermatogonia by GDNF. Science *287*, 1489–1493.

Mills, R.J., Parker, B.L., Quaife-Ryan, G.A., Voges, H.K., Needham, E.J., Bornot, A., Ding, M., Andersson, H., Polla, M., Elliott, D.A., et al. (2019). Drug screening in human PSC-cardiac organoids identifies pro-proliferative compounds acting via the mevalonate pathway. Cell Stem Cell *24*, 895–907.e896.

Morimoto, H., Ogonuki, N., Kanatsu-Shinohara, M., Matoba, S., Ogura, A., and Shinohara, T. (2021). Spermatogonial stem cell transplantation into nonablated mouse recipient testes. Stem Cell Reports *16*, 1832–1844.

Nurmio, M., Keros, V., Lähteenmäki, P., Salmi, T., Kallajoki, M., and Jahnukainen, K. (2009). Effect of childhood acute lymphoblastic leukemia therapy on spermatogonia populations and future fertility. JJ. Clin. Endocrinol. Metab. *94*, 2119–2122.

Oatley, J.M., and Brinster, R.L. (2012). The germline stem cell niche unit in mammalian testes. Physiol. Rev. *92*, 577–595.

Parekh, P.A., Garcia, T.X., and Hofmann, M.C. (2019). Regulation of GDNF expression in Sertoli cells. Reproduction *157*, R95–R107.

Parihar, S.P., Guler, R., and Brombacher, F. (2019). Statins: a viable candidate for host-directed therapy against infectious diseases. Nat. Rev. Immunol. *19*, 104–117.

Qian, C., Meng, Q., Lu, J., Zhang, L., Li, H., and Huang, B. (2020). Human amnion mesenchymal stem cells restore spermatogenesis in mice with busulfan-induced testis toxicity by inhibiting apoptosis and oxidative stress. Stem Cell Res. Ther. *11*, 290.

Rensen, S.S., Slaats, Y., Driessen, A., Peutz-Kootstra, C.J., Nijhuis, J., Steffensen, R., Greve, J.W., and Buurman, W.A. (2009). Activation of the complement system in human nonalcoholic fatty liver disease. Hepatology *50*, 1809–1817.

Sada, A., Hasegawa, K., Pin, P.H., and Saga, Y. (2012). NANOS2 acts downstream of glial cell line-derived neurotrophic factor signaling to suppress differentiation of spermatogonial stem cells. Stem Cells *30*, 280–291.

Sadaria, M.R., Reppert, A.E., Yu, J.A., Meng, X., Fullerton, D.A., Reece, T.B., and Weyant, M.J. (2011). Statin therapy attenuates growth and malignant potential of human esophageal adenocarcinoma cells. J. Thorac. Cardiovasc. Surg. *142*, 1152–1160.

Sasso-Cerri, E., Oliveira, B., de Santi, F., Beltrame, F.L., Caneguim, B.H., and Cerri, P.S. (2017). The antineoplastic busulphan impairs peritubular and Leydig cells, and vitamin B12 stimulates spermatogonia proliferation and prevents busulphan-induced germ cell death. Biomed. Pharmacother. *95*, 1619–1630.

Sharma, M., and Braun, R.E. (2018). Cyclical expression of GDNF is required for spermatogonial stem cell homeostasis. Development *145*, dev151555.

Shinohara, T., Orwig, K.E., Avarbock, M.R., and Brinster, R.L. (2001). Remodeling of the postnatal mouse testis is accompanied by dramatic changes in stem cell number and niche accessibility. Proc. Natl. Acad. Sci. USA *98*, 6186–6191.

Sun, F., Xu, Q., Zhao, D., and Degui Chen, C. (2015). Id4 marks spermatogonial stem cells in the mouse testis. Sci. Rep. *5*, 17594.

Tadokoro, Y., Yomogida, K., Ohta, H., Tohda, A., and Nishimune, Y. (2002). Homeostatic regulation of germinal stem cell proliferation by the GDNF/FSH pathway. Mech. Dev. *113*, 29–39.

Takashima, S., Kanatsu-Shinohara, M., Tanaka, T., Morimoto, H., Inoue, K., Ogonuki, N., Jijiwa, M., Takahashi, M., Ogura, A., and Shinohara, T. (2015). Functional differences between GDNF-dependent and FGF2-dependent mouse spermatogonial stem cell self-renewal. Stem Cell Reports *4*, 489–502.

Tan, K., Song, H.W., Thompson, M., Munyoki, S., Sukhwani, M., Hsieh, T.C., Orwig, K.E., and Wilkinson, M.F. (2020). Transcriptome profiling reveals signaling conditions dictating human spermatogonia fate in vitro. ProcProc. Natl. Acad. Sci. USA *117*, 17832–17841.

Tian, R., Yao, C., Yang, C., Zhu, Z., Li, C., Zhi, E., Wang, J., Li, P., Chen, H., Yuan, Q., et al. (2019). Fibroblast growth factor-5 promotes spermatogonial stem cell proliferation via ERK and AKT activation. Stem Cell Res. Ther. *10*, 40.

Tripathi, D.M., Vilaseca, M., Lafoz, E., Garcia-Caldero, H., Viegas Haute, G., Fernandez-Iglesias, A., Rodrigues de Oliveira, J., Garcia-Pagan, J.C., Bosch, J., and Gracia-Sancho, J. (2018). Simvastatin prevents progression of acute on chronic liver failure in rats with cirrhosis and portal hypertension. Gastroenterology *155*, 1564–1577.

Vakalopoulos, I., Dimou, P., Anagnostou, I., and Zeginiadou, T. (2015). Impact of cancer and cancer treatment on male fertility. Hormones *14*, 579–589.

von Kopylow, K., Kirchhoff, C., Jezek, D., Schulze, W., Feig, C., Primig, M., Steinkraus, V., and Spiess, A.N. (2010). Screening for biomarkers of spermatogonia within the human testis: a whole genome approach. Hum. Reprod. *25*, 1104–1112.

Wang, Z., Li, S., Wang, Y., Zhang, X., Chen, L., and Sun, D. (2019). GDNF enhances the anti-inflammatory effect of human adipose-derived mesenchymal stem cell-based therapy in renal interstitial fibrosis. Stem Cell Res. *41*, 101605.

Wu, X., Schmidt, J.A., Avarbock, M.R., Tobias, J.W., Carlson, C.A., Kolon, T.F., Ginsberg, J.P., and Brinster, R.L. (2009). Prepubertal human spermatogonia and mouse gonocytes share conserved gene expression of germline stem cell regulatory molecules. ProcProc. Natl. Acad. Sci. USA *106*, 21672–21677.

Xia, Y., Xie, Y., Yu, Z., Xiao, H., Jiang, G., Zhou, X., Yang, Y., Li, X., Zhao, M., Li, L., et al. (2018). The mevalonate pathway is a druggable target for vaccine adjuvant discovery. Cell *175*, 1059–1073.e1021.

Xu, H., Yang, Y.J., Yang, T., and Qian, H.Y. (2013). Statins and stem cell modulation. Ageing Res. Rev. *12*, 1–7.

Xu, J., Liu, X., Chen, J., Zacharek, A., Cui, X., Savant-Bhonsale, S., Liu, Z., and Chopp, M. (2009). Simvastatin enhances bone marrow stromal cell differentiation into endothelial cells via notch signaling pathway. Am. J. Physiol. Cell Physiol. *296*, C535–C543.

Yan, Y.L., Qiu, B., Hu, L.J., Jing, X.D., Liu, Y.J., Deng, S.B., Du, J.L., and She, Q. (2013). Efficacy and safety evaluation of intensive statin therapy in older patients with coronary heart disease: a systematic review and meta-analysis. Eur. J. Clin. Pharmacol. *69*, 2001–2009.

Yin, Y., Liu, L., Zhao, Z., Yin, L., Bauer, N., Nwaeburu, C.C., Gladkich, J., Gross, W., Hackert, T., Sticht, C., et al. (2018). Simvastatin inhibits sonic hedgehog signaling and stemness features of pancreatic cancer. Cancer Lett. *426*, 14–24.

Zeiser, R. (2018). Immune modulatory effects of statins. Immunology *154*, 69–75.

Zeiser, R., Maas, K., Youssef, S., Dürr, C., Steinman, L., and Negrin, R.S. (2009). Regulation of different inflammatory diseases by impacting the mevalonate pathway. Immunology *127*, 18–25.

Zhang, X., Wang, T., Deng, T., Xiong, W., Lui, P., Li, N., Chen, Y., and Han, D. (2013). Damaged spermatogenic cells induce inflammatory gene expression in mouse Sertoli cells through the activation of Toll-like receptors 2 and 4. Mol. Cell. Endocrinol. *365*, 162–173.

Zhang, X., Xia, Q., Wei, R., Song, H., Mi, J., Lin, Z., Yang, Y., Sun, Z., and Zou, K. (2019). Melatonin protects spermatogonia from the stress of chemotherapy and oxidation via eliminating reactive oxidative species. Free Radic. Biol. Med. *137*, 74–86.

Zohni, K., Zhang, X., Tan, S.L., Chan, P., and Nagano, M.C. (2012). The efficiency of male fertility restoration is dependent on the recovery kinetics of spermatogonial stem cells after cytotoxic treatment with busulfan in mice. Hum. Reprod. *27*, 44–53.

Stem Cell Reports, Volume *18*

Supplemental Information

Lovastatin promotes the self-renewal of murine and primate spermatogonial stem cells

Chaohui Li, Zhaokai Yao, Linzi Ma, Xiuling Song, Wen Wang, Cong Wan, Shaofang Ren, Dingyao Chen, Yi Zheng, Yong-tong Zhu, Gang Chang, Shihao Wu, Kai Miao, Fang Luo, and Xiao-Yang Zhao

Supplementary Information

Figure S1

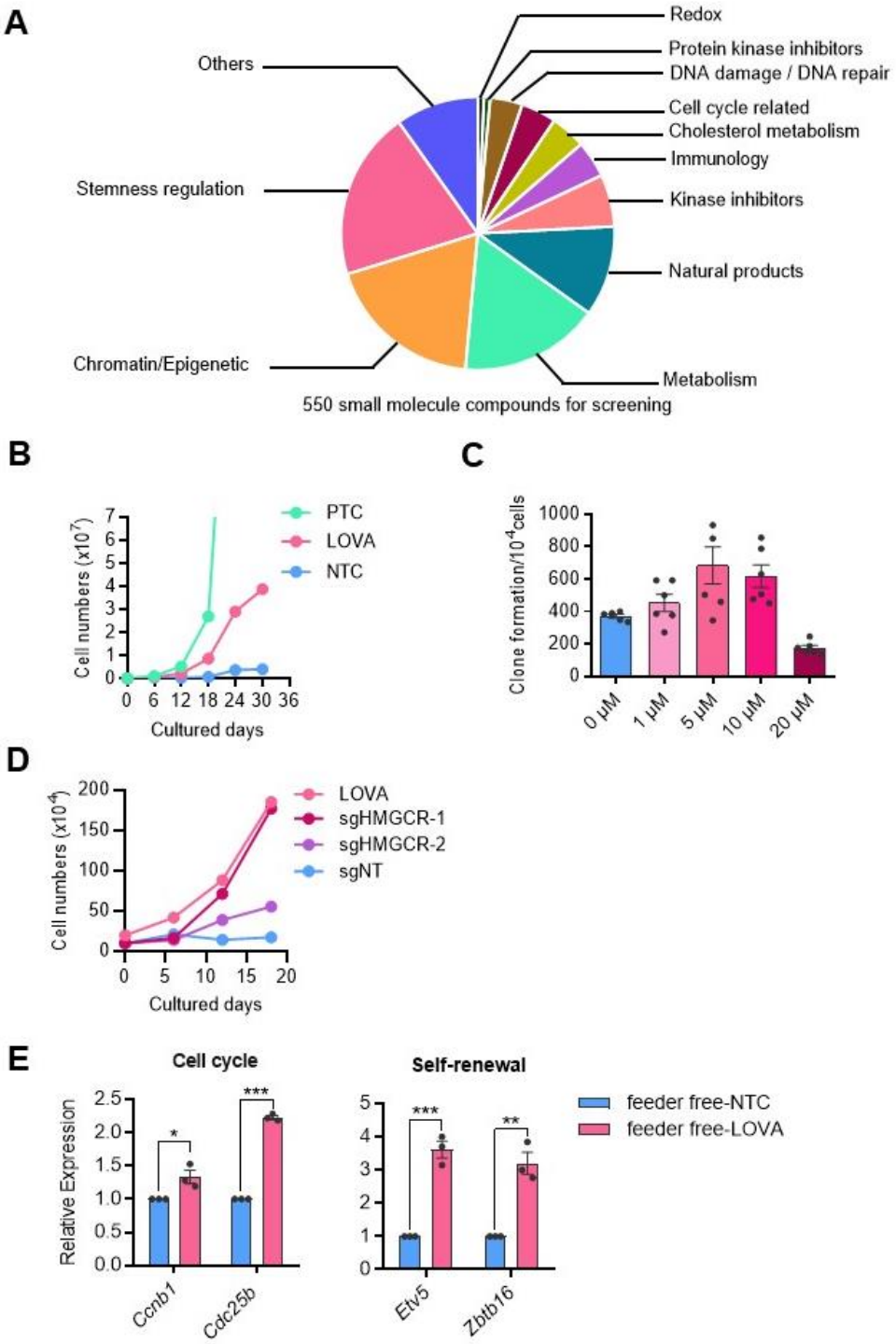

Figure S1. Small molecule screening for mSSCs self-renewal, related to Figure 1.

A) Classes of small molecule compounds tested.

B) Cell growth curve of *in vitro* cultured mSSCs in 3 different conditions.

C) Histogram of Lovastatin concentration gradient test. Error bars indicate mean ± SEM from five independent experiments.

D) Cell growth curve of *in vitro* cultured HMGCR knockdown of mSSCs cell lines and mSSCs from LOVA group (LOVA) was taken as the control.

E) qPCR analysis of mSSCs and undifferentiated spermatogonia cultured in feeder-free mSSCs culture system of NTC (feeder free-NTC) and LOVA (feeder free-LOVA) group. The relative expression levels of representative genes regarding cell cycle and self-renewal were assessed. Error bars indicate mean ± SEM from three independent experiments, **$p \leq 0.01$.

Figure S2

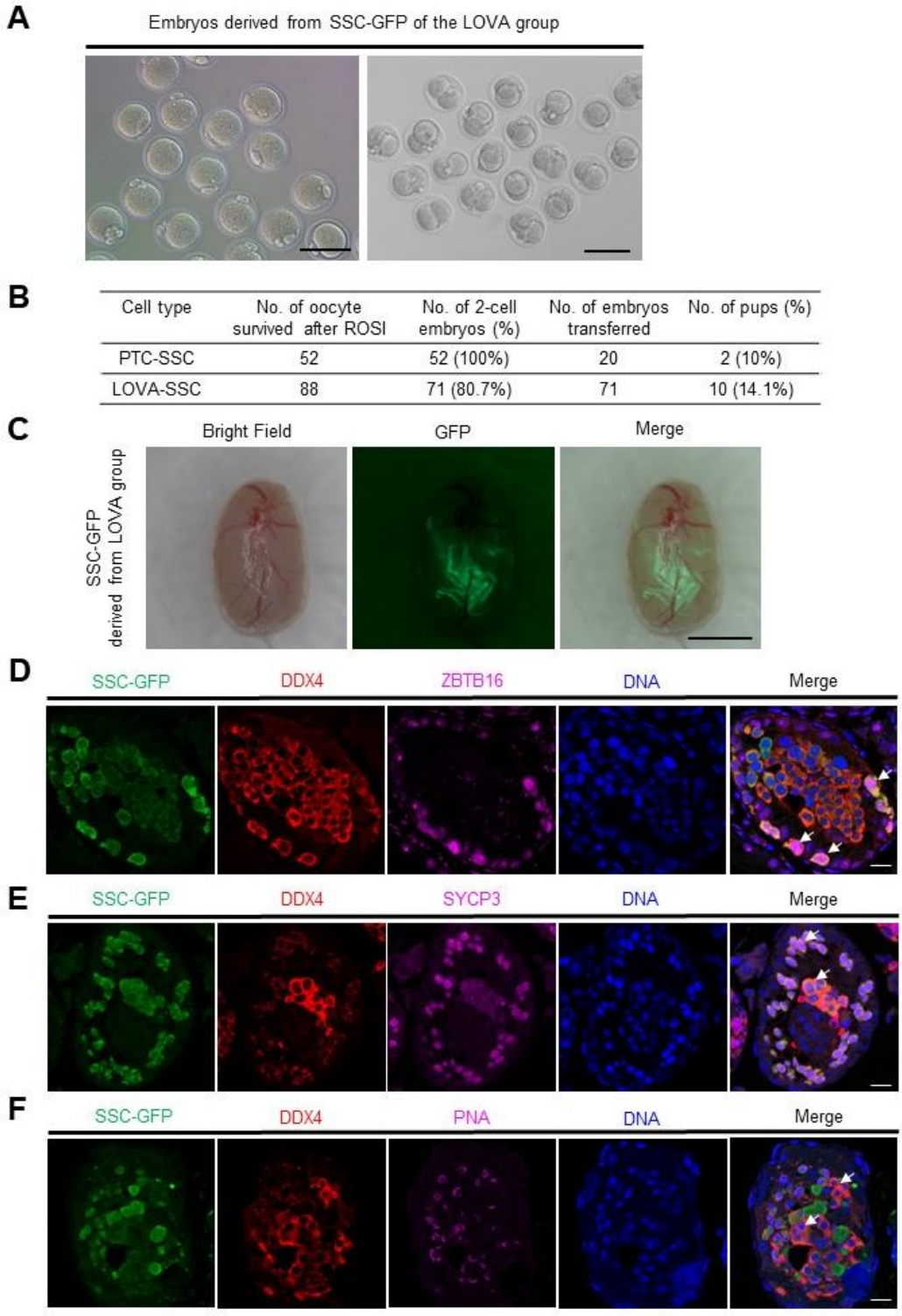

Cell type	No. of oocyte survived after ROSI	No. of 2-cell embryos (%)	No. of embryos transferred	No. of pups (%)
PTC-SSC	52	52 (100%)	20	2 (10%)
LOVA-SSC	88	71 (80.7%)	71	10 (14.1%)

Figure S2. Functional analysis of mSSCs from the LOVA group, related to Figure 2.

A) Photomicrographs of embryos at the pronuclear (left) or 2-cell (right) stage were injected with differentiated spermatids from LOVA derived SSC-GFP cells. Scale bars, 100 μm.

B) Statistics for embryo development and the generation of offspring from spermatids derived from SSC-GFP from the PTC (PTC-SSC) or LOVA (LOVA-SSC) group, respectively.

C) Macroscopic appearance of busulfan-treated adult mouse recipient testes that were transplanted with SSC-GFP derived from LOVA condition. Scale bar, 2 mm.

D, E, F) Immunofluorescent staining of busulfan-treated adult mouse recipient testes that were transplanted with SSC-GFP derived from LOVA condition. ZBTB16 (D), SYCP3 (E), and PNA (F) were labeled as markers of undifferentiated spermatogonia, spermatocyte, and spermatid, respectively. DDX4 was used as the germ cell marker. Scale bars, 20 μm.

Figure S3

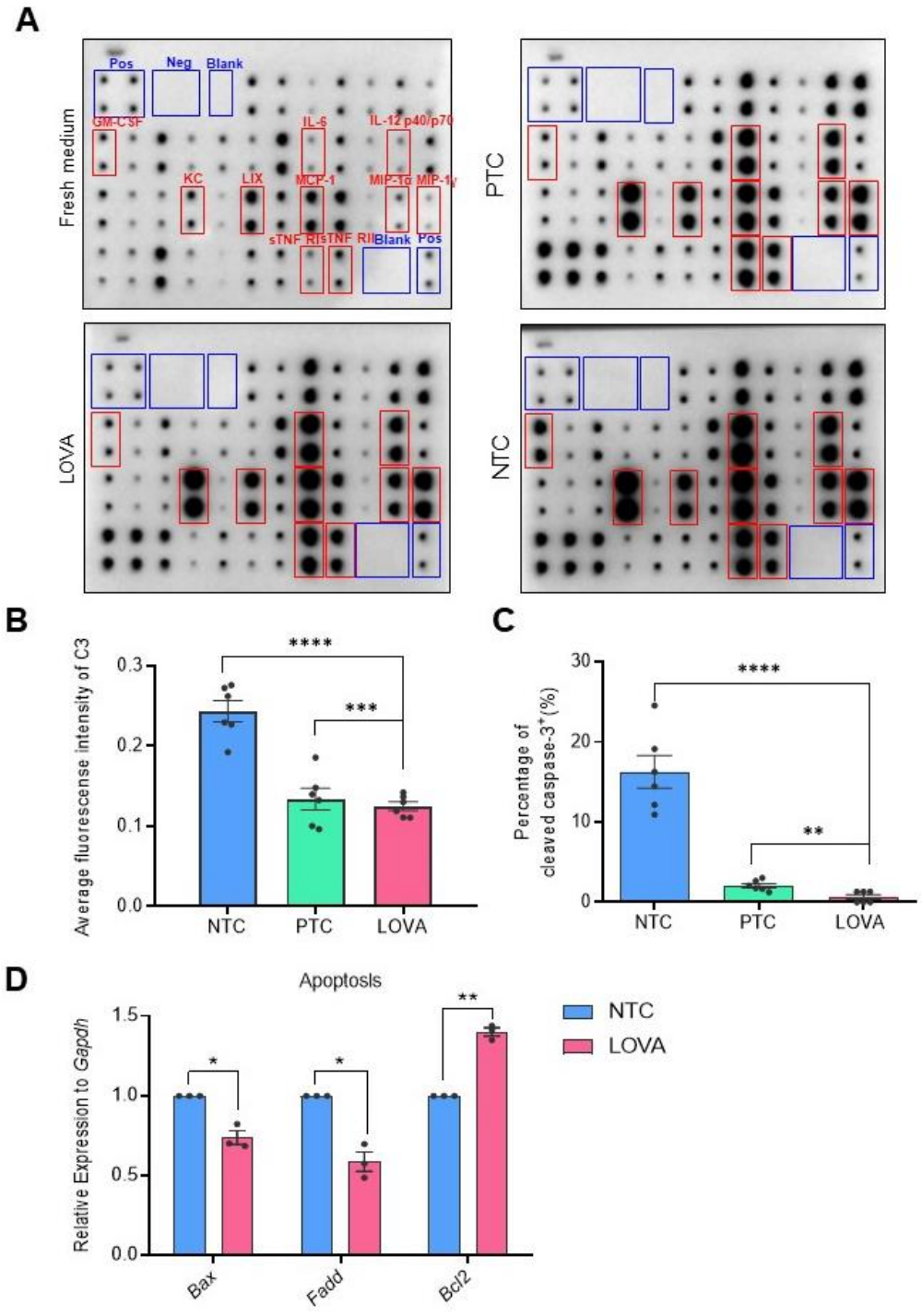

Figure S3. Levels of cytokines and apoptosis were reduced in LOVA, related to Figure 3.

A) Cytokine array analysis. Blue box labeled control of this assay. Red box labeled inflammatory factors which significantly upregulated in LOVA groups compared to the fresh medium group.

B) Statistics of average fluorescence intensity of complement 3 in cell clones cultured in 3 different conditions. Error bars indicate mean ± SEM from six independent experiments, ***p≤0.001, ****p≤0.0001.

C) Statistics of cleaved caspase-3^{+} cells in cell clones cultured in 3 different conditions. Error bars indicate mean ± SEM from six independent experiments, **p≤0.01, ****p≤0.0001.

D) qPCR analysis of the relative expression level of representative genes regarding apoptosis. Error bars indicate mean ± SEM from three independent experiments, *p≤0.05, **p≤0.01.

Figure S4

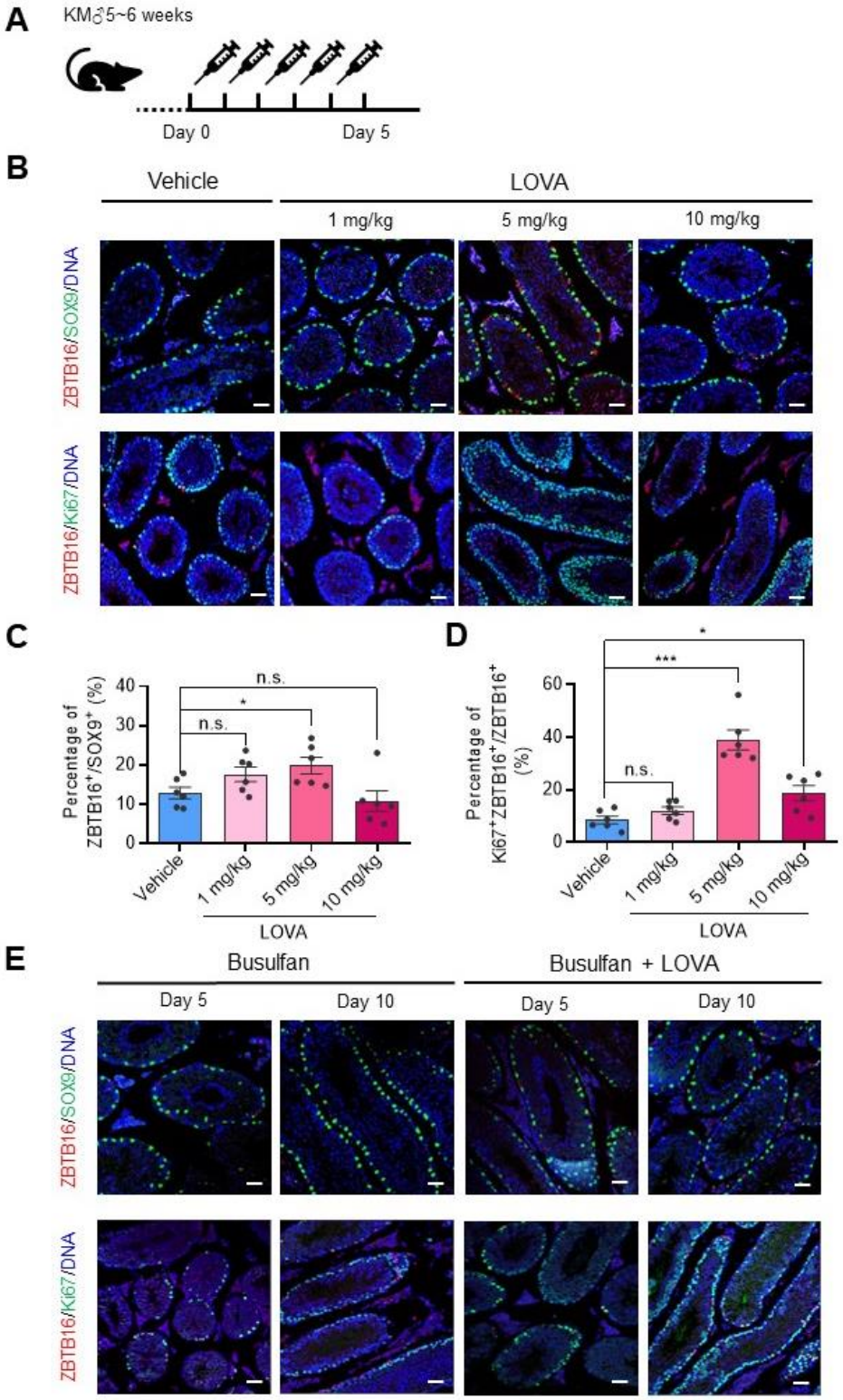

Figure S4. Lovastatin could promote the regeneration of undifferentiated spermatogonia *in vivo*, related to Figure 5.

A) Schematic outline of LOVA injection under physiological conditions.

B) Immunofluorescent staining of undifferentiated spermatogonia marker (ZBTB16) and Sertoli cell marker (SOX9) or cell proliferation marker Ki67 expression in mouse testis treated with Lovastatin under physiological conditions. Scale bars, 50 μm.

C) Histogram calculation of the proportion of undifferentiated spermatogonia ($ZBTB16^+$ cells) compared to Sertoli cells ($SOX9^+$ cells) in B) from six independent experiments. Error bars indicate mean ± SEM, *p≤0.05, ns, non-significant.

D) Histogram calculation of the proportion of proliferative undifferentiated spermatogonia ($Ki67^+ZBTB16^+$ cells) compared to total undifferentiated spermatogonia ($ZBTB16^+$ cells) in B) from six independent experiments. Error bars indicate mean ± SEM, *p≤0.05, ***p≤0.001, ns, non-significant.

E) Immunofluorescent staining of spermatogonia marker (ZBTB16) and Sertoli cell marker (SOX9) or cell proliferation marker (Ki67) in mouse testis under chemotherapy condition. Scale bars, 50 μm.

Table S1: List of primers used in RT-qPCR, related to Figure 3 and Figure4.

Gene name	Forward primer sequence	Reverse primer sequence
Gapdh	TGTGTCCGTCGTGGATCTGA	TTGCTGTTGAAGTCGCAGGA
Zbtb16	CTGGGACTTTGTGCGATGTG	CGGTGGAAGAGGATCTCAAACA
Etv5	TCAGTCTGATAACTTGGTGCTTC	GGCTTCCTATCGTAGGCACAA
C-kit	GCCACGTCTCAGCCATCTG	GTCGCCAGCTTCAACTATTAACT
Cd68	TGTCTGATCTTGCTAGGACCG	AGGAGAGTAACGGCCTTTTTG
Apoe	GACCCAGCAAATACGCCTG	CATGTCTTCCACTATTGGCTCG
Ccnb1	GCGTGTGCCTGTGACAGTTA	CCTAGCGTTTTTGCTTCCCTT
Cdc25b	TCCGATCCTTACCAGTGAGG	GGGCAGAGCTGGAATGAGG
Bax	CCGGCGAATTGGAGATGAACT	CCAGCCCATGATGGTTCTGAT
Bcl2	ATGCCTTTGTGGAACTATATGGC	GGTATGCACCCAGAGTGATGC
Fadd	GCGCCGACACGATCTACTG	TTACCCGCTCACTCAGACTTC

Supplemental Experimental Procedures

Animal and human tissues

Mouse experiments were performed in the Animal Experimental Center of Southern Medical University under the approval for animal studies by the competent institution. Cynomolgus monkeys (*Macaca fascicularis*) were purchased from Guangdong Institute of Biological Resources Application which has been approval for animal studies by the competent institution.

All human samples related experiments were carried out in accordance with The Code of Ethics of the World Medical Association. The medical ethics committee of Southern medical university is No. NFEC-2019-219. The materials used in the experiment were from 2 patients with obstructive azoospermia, and the patients were informed of the purpose of the experiment.

mSSC cell line establishment

Testicular cells were derived from CAG-GFP transgenic C57/DBA mice on day 3 after birth as previously described (Kanatsu-Shinohara et al., 2003). In brief, testicular tissue was cut into small pieces then digested with collagenase IV (1 mg/ml; Invitrogen) for 15 min, followed by 0.25% trypsin/1 mM EDTA digestion (Invitrogen) for 10 min. Cells were resuspended in αMEM with 10% FBS then inoculated in 0.1% gelatin-coated culture dishes for 24 hours to separate the germ cells from the somatic cells. Purified germ cells were cultured on Mitomycin-treated mouse embryonic fibroblasts (MEFs) for long-term propagation. For the basic culture medium, StemPro-34 SFM (Invitrogen) supplemented with 1% FBS, 0.1 mM NEAA, 1 mM sodium pyruvate, 2 mM GlutaMAX, 100 U/mL penicillin, 0.1 mg/mL streptomycin, 50 μM β-mercaptoethanol, 1 μL/mL DL-lactic acid, 1 × minimal essential medium (MEM) Vitamin Solution, 10 μg/mL biotin, 100 μM ascorbic acid, 60 ng/mL progesterone, 30 ng/mL β-estradiol, 6 mg/mL Glucose, 5 mg/mL Bovine

Serum Albumin (BSA), and 1% N2 supplement. PTC group culture medium contains 10 ng/mL recombinant rat GDNF (R&D Systems, 512-GF), 10 ng/mL recombinant mouse EGF (R&D Systems, 2028-EG), 5000 U recombinant mouse LIF (Millipore, ESG1107), and 10 ng/mL recombinant mouse FGF2 (R&D Systems, 3139-FB). The difference between NTC and PTC group culture medium is the presence of GDNF. The LOVA group culture medium replaces GDNF with 5 μM Lovastatin (TargetMol, T1207). For feeder-free culture system, long-term propagated mSSCs were cultured on dishes coated with 20 mg/ml laminin (BD Biosciences) as previously described (Kanatsu-Shinohara et al., 2011). The feeder-free culture medium was supplemented with B27 (Invitrogen) with basic culture medium described above. The culture medium was changed every other day and the subcultivation ratio of 1:3-5 per week was used.

mSSCs *in vivo* transplantation and Intracytoplasmic Sperm Injection

The day12.5 pregnant ICR mouse was used to generate the recipient male pups. The pregnant mice were treated with 40 mg/kg busulfan by intraperitoneal injection. Testicular transplantation of mSSCs was performed on the newborn male pups at 5-10 days postpartum. Anesthesia the recipient and split the hypogastrium to pull out testis. Prepare a glass needle with a 40 μm inner diameter. Fill the needle with 2×10^5 cell/μL mSSC cell suspension and add a small amount of trypan blue at the tip of the needle. Found the output tubules, which along the parallel direction of the testicular artery under the microscope, then poked the needle into the output tubules and inserted into the direction of the testicular reticulum along the output tubules, then blown the cells into the seminiferous tubules of the testis. After injection, Place the testicles and fat pads back into the abdominal cavity carefully and avoid torsion of the testicles. Sutured abdominal wound layer by layer. Finally, alcohol cotton was applied to the abdomen of the mice to prevent infection. The mice were placed in the worm table at 37°C. Then put them back into

the feeding room while woke up. 2 months after SSC transplantation, the testicular tissue from recipient mice was digested into single cells suspension and stained with 10 mg/mL Hoechst 33342 for 20 min and washed three times with PBS. The haploid spermatids with GFP fluorescence from the CAG-EGFP transgenes were collected by loading on a MoFlo XDP (Beckman Coulter). The cell suspension was kept at 4°C until ROSI. The ROSI was performed essentially as described previously (Kishigami and Wakayama, 2007).

RNA isolation and library preparation

SSC cells were collected after 18 days cultured in different conditions. Total RNA isolation and Illumina transcriptome sequencing library preparation were performed according to the manufacturer's instructions with the NEB Next Ultra II Directional RNA Library Prep Kit (NEB, E7760L). The constructed NGS libraries were sequenced with Illumina Hiseq XTEN platform at Novogene and sequencing strategy was paired-end 150 bp (PE150).

Transcriptome data analysis

The total reads were quality- and adapter-trimmed using BBDuk and Trimmomatic (v0.38) (Bolger et al., 2014). The mouse transcriptome index was generated using the reference genome mm10 with Ensembl version 95 and the clean reads were aligned to mm10 transcriptome using RSEM (Li and Dewey, 2011) integrated Bowtie2 (v 2.4.1) (Langmead and Salzberg, 2012). Gene counts were calculated using RSEM. To ensure data quality, the low expressed genes which counts did not >=50 in at least two samples were eliminated for following analysis. R-Bioconductor package DESeq2 (Love et al., 2014) was used to normalized count data and calculated differentially expressed genes across different groups ($P< 0.05$).

Testicular tissue paraffin-embedded section

The testicular tissue was washed twice with PBS then fixed in 4% paraformaldehyde overnight at 4°C after. The fixed tissue was transferred to the embedding frame and dehydrated with 70%, 80% and 90% ethanol solution successively, followed by 100% alcohol and xylene transparent sample successively, and then paraffin penetration. FFPE sample was sectioned into 5-7 μm pieces and pasted on slide for further use.

Statistics and Reproducibility

Microsoft Excel, GraphPad Prism (version 8.0.1) and R (version 3.5.1) software were used for statistical calculations. Specific statistical tests, sample number and other information are indicated in the main text or figure legends. The t-test and two-sided statistical analysis approach was used to determine the significance of the difference between the different sets of data if there was no specific indication. All experiments were conducted at least two times independently, and similar results were adopted for further analysis to guarantee reproducibility.

Immunostaining

mSSCs cultured on the glass slides were fixed with 4% paraformaldehyde after clone formation. Then the sample was permeated with PBS containing 0.5% TritonX-100 for 20 min and blocked with 2% BSA for 1 hour at room temperature.

The testicular tissue sections were re-hydrated gradually in Xylene and serial concentrations (100%, 90%, 80%, and 70%) of ethanol. Then the tissue sections were boiled at 95°C for 10 min in EDTA antigen retrieval solution (pH 8.0) and followed by 30 min incubation at room temperature then block the slides with 2% BSA for 1 hour. After finished the blocking, the primary antibody was added to the sample and incubation at 4°C overnight. Wash the sample with PBS 3 times, and then the corresponding secondary Immunofluorescence

antibody and Hoechst33342 were added for incubation at room temperature for 1 hour. Wash the samples in PBS 3 times. Finally, the section was sealed using anti fluorescence quenching agent and the confocal microscope (Carl Zeiss) was used for further detection. At least 3 fields were calculated in each experiment.

Cas13d-mediated HMGCR knockdown

The knockdown of HMGCR was conducted by using CRISPR/Cas13d system. Two sgRNAs designed to target the coding sequence of HMGCR mRNAS were prepared：

sgHMGCR-1F	AAACAACACAAAGTAGTTGGCCAACAC
sgHMGCR-1R	AAAAGTGTTGGCCAACTACTTTGTGTT
sgHMGCR-2F	AAACACACAAAGTAGTTGGCCAACACT
sgHMGCR-2R	AAAAAGTGTTGGCCAACTACTTTGTGT

Non-targeting sgRNA (sgNT) for control was used as previously described (He et al., 2020). According to previous reports (He et al., 2020; Konermann et al., 2018), lentivirus packaging and transfection were performed.

Western blot

Cells were lysed in RIPA Lysis buffer (R0010, Solarbio) to collect the cellular proteins, which were resolved by SDS-PAGE and transferred to PVDF membrane (RPN303F, GE), blocked, probed with the primary antibody target HMGCR (ab174830, abcam) and the secondary antibody (KM9007, Sungene). Immuno-reactive bands were visualized using the ECL Western Blotting Substrate Kit (YEASON, 36208ES60) before exposure. The intensities of bands were quantified with ImageJ software (http://imagej.nih.gov/ij/).

Quantitative real-time PCR analysis

SSC samples were collected after 18 days cultured in different conditions and total RNA was extracted using Trizol reagent (TIANGEN, DP424) according to the manufacturer's instructions. RNA was subsequently reversely transcribed

to cDNA using the HiScript Q RT SuperMix Kit (Vazyme, R123-01). Then cDNA was diluted and used for RT-qPCR with RealStar Green Fast Mixture reagent (GenStar, A301-101) and designed primers on a LightCycler®96 (Roche, 900012C). Every sample has triplications and the relative mRNA expression levels of targeted genes were calculated through the $2^{-\Delta\Delta CT}$ method after normalized by housekeeping gene *Gapdh*. The detailed sequence of primers was listed in Table S1.

Supplemental References

Bolger, A.M., Lohse, M., and Usadel, B. (2014). Trimmomatic: a flexible trimmer for Illumina sequence data. Bioinformatics *30*, 2114-2120.

He, B., Peng, W., Huang, J., Zhang, H., Zhou, Y., Yang, X., Liu, J., Li, Z., Xu, C., Xue, M., *et al.* (2020). Modulation of metabolic functions through Cas13d-mediated gene knockdown in liver. Protein Cell *11*, 518-524.

Kanatsu-Shinohara, M., Inoue, K., Ogonuki, N., Morimoto, H., Ogura, A., and Shinohara, T. (2011). Serum- and feeder-free culture of mouse germline stem cells. Biol Reprod *84*, 97-105.

Kanatsu-Shinohara, M., Ogonuki, N., Inoue, K., Miki, H., Ogura, A., Toyokuni, S., and Shinohara, T. (2003). Long-term proliferation in culture and germline transmission of mouse male germline stem cells. Biol Reprod *69*, 612-616.

Kishigami, S., and Wakayama, T. (2007). Efficient strontium-induced activation of mouse oocytes in standard culture media by chelating calcium. J Reprod Dev *53*, 1207-1215.

Konermann, S., Lotfy, P., Brideau, N.J., Oki, J., Shokhirev, M.N., and Hsu, P.D. (2018). Transcriptome Engineering with RNA-Targeting Type VI-D CRISPR Effectors. Cell *173*, 665-676 e614.

Langmead, B., and Salzberg, S.L. (2012). Fast gapped-read alignment with Bowtie 2. Nat Methods *9*, 357-359.

Li, B., and Dewey, C.N. (2011). RSEM: accurate transcript quantification from RNA-Seq data with or without a reference genome. BMC Bioinformatics *12*, 323.

Love, M.I., Huber, W., and Anders, S. (2014). Moderated estimation of fold change and dispersion for RNA-seq data with DESeq2. Genome Biol *15*, 550.